

Dynamics of the cell coat and cell membrane complex
accompanied by locomotion of *Amoeba proteus*

2 0 1 3

Atsushi Taniguchi

Contents

| | |
|---|----|
| Summary | 1 |
| General Introduction | 2 |
| Chapter I: Behavior of glycocalyx during locomotion | 8 |
| 1.1 Abstract | 9 |
| 1.2 Introduction | 10 |
| 1.3 Materials and Methods | 12 |
| 1.4 Results | 13 |
| 1.5 Discussion..... | 15 |
| 1.6 Figures | 17 |
| Chapter II: Dynamics of cell surface and cytoplasm | 24 |
| 2.1 Abstract | 25 |
| 2.2 Introduction | 26 |
| 2.3 Materials and Methods | 29 |
| 2.4 Results and Discussion | 31 |
| 2.5 Figures | 36 |
| Chapter III: Three-dimensional analysis of amoeboid movement | 39 |
| 3.1 Abstract | 40 |
| 3.2 Introduction | 41 |
| 3.3 Materials and Methods | 45 |
| 3.4 Results and Discussion | 47 |
| 3.5 Figures | 49 |
| General Discussion | 52 |
| Appendix | 55 |
| References | 58 |
| Acknowledgement | 63 |

Summary

The plasma membrane dynamics of *Amoeba proteus* is considered essential for amoeboid movements, but remains unclear. To obtain mechanical insight into the membrane dynamics, which enables flexible amoeboid movement, it is essential to understand overall flow of plasma membrane during amoeboid movement. In this thesis, I utilized a new technique, Digital Scanned Light-sheet Microscopy at high speed and observed cell surface dynamics visualized by 1,1'-dioctadecyl-3,3,3',3'-tetramethylindocarbocyanine perchlorate staining and cytoplasmic flow represented by mitochondria labeled with MitoTracker Deep Red. Such observation revealed that both ventral and dorsal cell surfaces of a pseudopod move to extending direction, while the surface of posterior region does not. Three-dimensional observation using ezDSLIM, leads to the similar conclusion that in the ventral, dorsal and lateral cell surfaces of the pseudopod move forward extending direction continuously. These observations suggest that the plasma membrane dynamics of *A. proteus* can be explained by the total folding and unfolding model. I also found that the cell surface in the uroid rotates upon its retraction while the cytoplasmic gel relatively static against the substrate.

The cell surface of pseudopod moves to the locomoting direction, whereas mitochondria in the cytoplasmic gel rear the surface does did not move for the substrate. This result strongly indicates that the sliding between the plasma membrane and the cytoplasmic gel occurs. Nishigami (2013) showed that sol-gel conversion can be elicited by shear stress, suggesting that the sol-state between the plasma membrane and the cortical cytoplasmic gel might be induced by forward movement of the plasma membrane. Indeed, cytoplasmic flow could be observed beneath the plasma membrane in locomoting *A. proteus*.

General Introduction

Amoeboid movement, which is defined as a locomoting mode accompanied with cell shape change and crawling over the substrate, is observed in a variety types of cells, such as Sarcodina, Mycetozoa, fish keratocyte, mammalian leukocyte, fibroblasts, etc. despite the fact that these cells have no apparent motile apparatus (Lämmermann and Sixt 2009). Two modes of mechanisms underlying this type of movement are known. One is actin assembly-dependent mode (Svitkina and Borisy 1999, Pollard 2003), and the other is actomyosin-dependent mode (Charras *et al.* 2005, Charras and Paluch 2008). In the former, actin assembly in the pseudopod pushes the plasma membrane in the leading region, and in the latter, contraction of actomyosin in the posterior region generates hydrostatic pressure, which pushes the plasma membrane. Some types of cells are known to use both types of mechanisms according to their environments (Yoshida and Soldati 2006, Ley *et al.* 2007).

A free-living giant amoeba, *Amoeba proteus* has long attracted many biologists because of its large size and vigorous movement, which were strong advantages in observing the specimens with old-type light microscopes. In 1960-1980, there was a big debate over the mechanism of its movement, especially over that of the motive force generation. First, people thought that the gel layer just under the plasma membrane contract, and the resultant hydrostatic pressure pushes the cytoplasmic sol forward (the tail contraction hypothesis) (Mast 1926, Goldacre 1964, Opas 1976, Rinaldi and Opas 1976). In 1960, however, Allen observed vigorous cytoplasmic flow in the open cytoplasm in which two parts of an amoeba cell were demembrated by breaking the both ends of a narrow glass capillary filled with an amoeba cell. He insisted that motive force for the cytoplasmic flow in amoeba is generated in the absence of the closed membrane to maintain hydrostatic pressure and proposed a new hypothesis, the frontal contraction hypothesis (Allen 1961, Talor *et al.* 1973). Nowadays, the tail contraction hypothesis is mostly accepted in various amoeboid movement, and this mode is thought to be involved in bleb-dependent motility (Fackler and Grosse 2008). While the mode of amoeboid movement in *A. proteus* is still under debate.

During amoeboid movement, the plasma membrane plays a pivotal role, because it must move against the substrate for cell locomotion. However,

how the plasma membrane moves during amoeba locomotion is still an open question. Several models of the dynamics of the plasma membrane in amoeboid movement, have been proposed. Three major models are described below.

Rolling motion model: The plasma membrane performs the endless track locomotion (Mast 1926, Griffin and Allen 1960, Abe 1962, Seravin 1964). The dorsal membrane moves forward until it arrives at the anterior edge and turns to the ventral membrane. The ventral membrane stays attaching to the substrate and moves toward the dorsal side at the posterior edge (Fig. 1). In the observation of *Vannella* (fan-shaped amoeba), latex beads attached to the plasma membrane moved like this model (Hulsmann 1972). Thus, it is presumed that the plasma membrane dynamics of *Vannella* is rolling motion.

Retrograde Lipid Flow (RLF) model: The plasma membrane is sequestered in the posterior region by endocytosis, delivered forward, and fused at the anterior region by exocytosis (Bell 1961, Goldacre 1961, 1964). Both dorsal and ventral plasma membranes do not move against the substrate (Fig. 2).

Physarum (Mycetozoa) is considered to move according to this model because active exocytosis coupled with locomotion was observed (Sesaki and Ogihara 1997).

Total Folding and Unfolding (TFU) model: The folding of plasma membrane is formed by the contraction in the posterior region, and the plasma membrane area corresponding to the folded area is transferred to the leading edge to be used for pseudopod expansion (Czarska and Grebecki 1966). Both dorsal and ventral plasma membranes moved forward except at the adhesion sites which attach to the substrate in the ventral membrane (Fig. 3).

There are several reports arguing the mode of the cell surface movement in *A. proteus*. Some studies suggested, through electron microscopic observations, that the plasma membrane occurs exocytosis, and endocytosis may contribute to membrane movement during the locomotion in *A. proteus* (Wohlfarth-Bottermann and Stockem 1966, Stockem 1969 1972). However, these observations do not tell precise direction and flow of cell surface during the endocytosis and exocytosis, and it is difficult to estimate how much of membranes can be supplied by this system. It might not reflect the living cell locomotion because of the fixed cell images. There are investigations that tracked the markers attached to the plasma membrane of *A. proteus* (Haberey *et al.* 1969, Haberey 1970, Grebecki 1986). According to

these observations, the markers moved forward in the pseudopod, but stayed at the folds in the posterior region to support the TFU model. Komnick (1973) proposed that the plasma membrane of *A. proteus* employed both the TFU and RLF models. Although the plasma membrane dynamics has been observed well at both dorsal and lateral regions, few studies at the ventral region has been carried out. Indeed, movement of the ventral membrane is an essential piece of information to distinguish between the rolling motion model and the total folding and unfolding model. Therefore, the conclusion has not been obtained yet.

To clarify the dynamics of the plasma membrane in every region of *A. proteus*, I carried out the observation of both ventral and dorsal surfaces using staining of 1,1'-dioctadecyl-3,3,3',3'-tetramethylindocarbocyanine perchlorate (DiI) for the cell surface, that of MitoTracker Deep Red for the cytoplasm and a new microscopic technique, (Digital Scanned Light-sheet Microscopy) DSLM for the observation of the sectioned view of living cell. I improved the DSLM for high-speed three-dimensional observation, ezDSLM, and observed the three-dimensional plasma membrane dynamics of *A. proteus* by the ezDSLM.

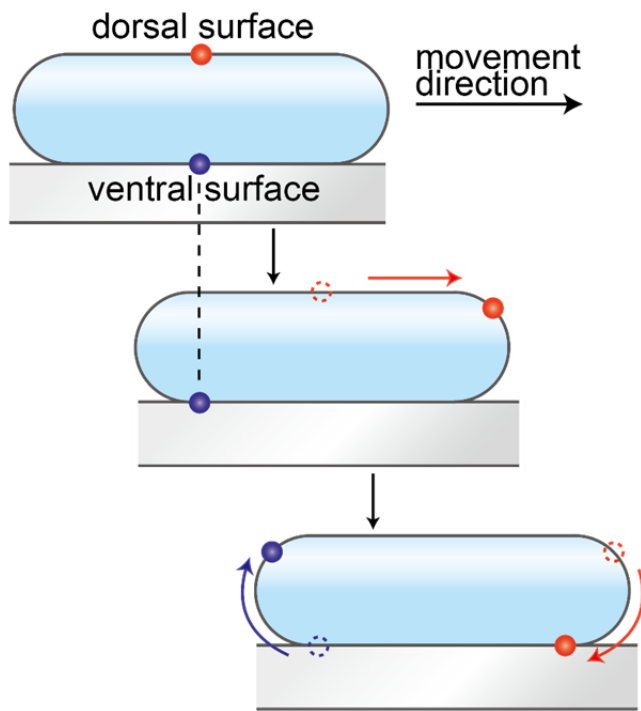


Fig. 1 Rolling motion model

The above scheme shows indicate plasma membrane dynamics of the rolling motion model. Red circle, a part of the dorsal plasma membrane; blue circle, a part of the ventral membrane; dashed circle, a position of before movement. The dashed line shows the same position on the substrate (Modified from Komnick, *et al.* 1973).

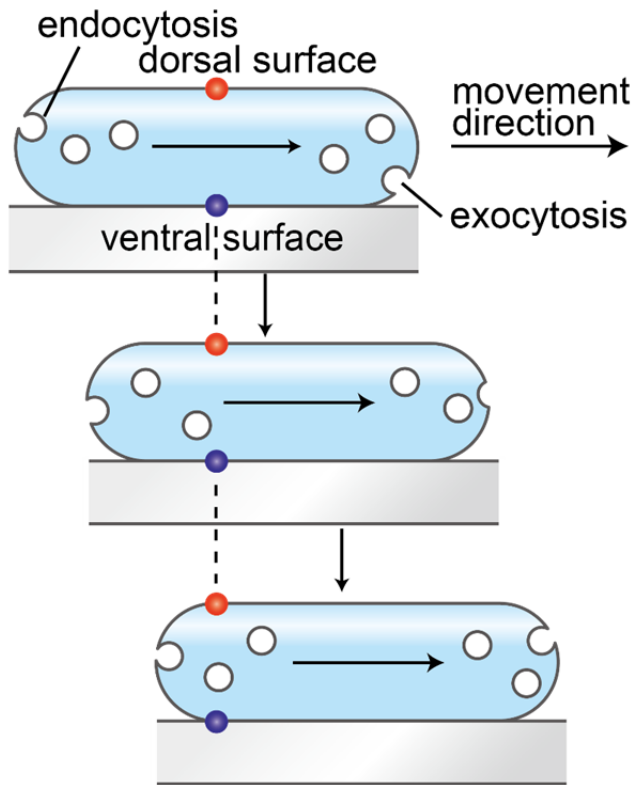


Fig. 2 Retrograde lipid flow model (RLF model)

A scheme showing plasma membrane dynamics of the RLF model. Red circle, a part of the dorsal plasma membrane; blue circle, a part of the ventral membrane (Modified from Komnick, et al. 1973).

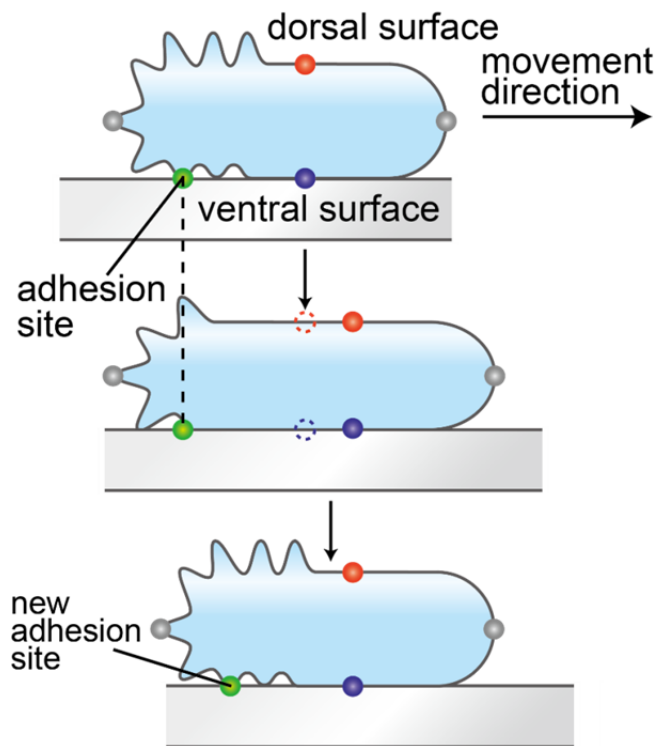


Fig. 3 Total folding and unfolding mode (TFU model)

A scheme shows the plasma membrane dynamics of the TFU model. Red circle, a part of the dorsal plasma membrane; blue circle, a part of the ventral membrane; gray circle, posterior and anterior edges; dashed circle, and a position of each membrane part before movement. The dashed line shows a membrane part attached to the substate (Modified from Komnick, et al. 1973).

Chapter I

Behavior of glycocalyx during locomotion

Abstract

To elucidate the plasma membrane dynamics, *Amoeba proteus* was stained with Alexa 488 concanavalin A (Con A) which binds to the glycocalyx of the amoeba surface, and recycling of the glycocalyx during cell movement was monitored. Fluorescence intensity at the pseudopod edge did not change during locomotion, and the fluorescence was not found in the cytoplasm in 0.3 h incubation. These observations are against the RLF model. Incidentally, the prolonged incubation of cells led to incorporation of some Con A. Incorporation of Con A during this long incubation significantly increase by adding 2% egg albumin which is an inducer of pinocytosis for *A. proteus* while the activation of pinocytosis did not after pseudopod formation in *A. proteus*.

These results also indicate that endocytosis and exocytosis have only minor contribution to membrane dynamics during amoeboid movement.

Next, movement of a particular position of the cell surface was examined by monitoring charcoal particles attached to cell surface. Particles in the lateral and Uorsal region of pseudopods moved forward during locomotion, while these at the anterior and posterior edges stayed at the same position. Those observations suggest that plasma membrane dynamics of *A. proteus* can be explained by the TFU model.

Introduction

By light microscope, the cell membrane of *A. proteus* appears thick. It is called “plasmalemma”, which the glycocalyx and the lipid bilayer. The plasmalemma of *A. proteus* consists of three layers; a filamentous layer of long sugar chains, an amorphous layer with the honeycomb structure and the plasma membrane of a lipid bilayer. (Mast 1925, Hausmann and Stockem 1972, Page 1986, Smirnov *et al.* 2005). These observations show that the glycocalyx linked with the plasma membrane. Therefore, the glycocalyx is thought to move together with the plasma membrane during locomotion of *A. proteus*.

Preceding studies have proposed some models for plasma membrane dynamics in *A. proteus*, but it is still not clear as stated in General Introduction. To approach this dynamics, I first examined dynamics of the glycocalyx using a fluorescently labeled concanavalin A, a lectin that can bind the glycocalyx *A. proteus*. The exocytosis and endocytosis of the glycocalyx can be observed by this fluorescence because the amoeba cell uniformly stains with it. Next, the amoeba cell surface of amoeba was labeled with charcoal particles, and the portion of the cell surface were visualized in the amoeba cell by these particles. I evaluated the rolling motion, RLF and TFU models by these observations.

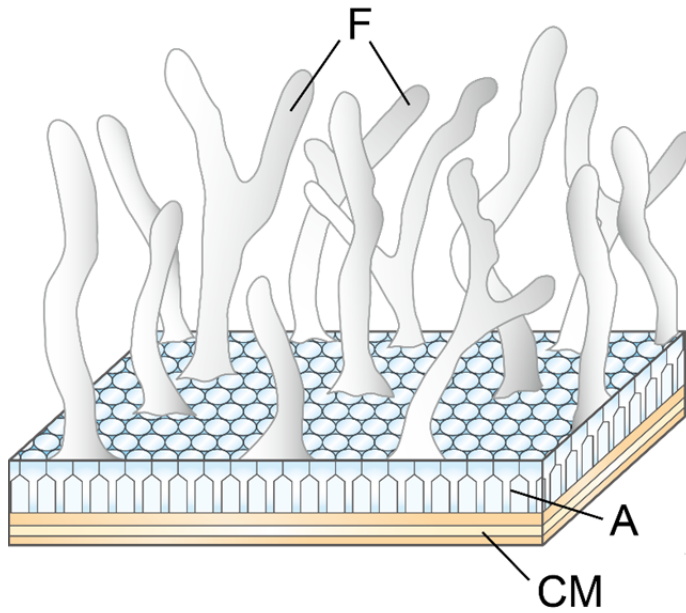


Fig. 4 The structure of the cell surface of *A. proteus*

A schematic illustration of “plasmalemma”. F, filamentous layer of glycocalyx; A, amorphous layer, CM, plasma membrane (Modified from Komnick, *et al.* 1973).

Materials and Methods

Cell culture

A. proteus was cultured in plastic boxes (30 x 22 x 5 cm) filled with the KCM medium (9.39 μ M KCl, 32.5 μ M MgSO₄·7H₂O, 54.4 μ M CaCl₂·2H₂O) at 25 °C, and feeded with *Tetrahymena pyriformis* twice a week. *T. pyriformis* was cultured 2 %(w/v) Bacto Proteose Peptone (Becton, Dickinson and Company, NJ, USA,) medium for three days. Cells were starved for at least three days before experiments.

Staining of the glycocalyx

The glycocalyx of *A. proteus* was stained with 5 μ g/ml Concanavalin A, Alexa Fluor 488 conjugate (Alexa488 Con A) (Invitrogen, CA, USA) for five minutes, and cells were washed three times with the fresh medium. Subsequently, cells were put in a chamber on a glass slide with an approximate thickness of 200 μ m. Samples were observed with a fluorescence microscope. To induce pinocytosis, cells were treated with 2 %(w/v) egg albumin.

Observation of the cell surface with charcoal particles

Charcoal particles that were ground with a mortar were applied to the amoeba sample mounted in a observation chamber filled with of the KCM medium.

Microscopy

A fluorescence microscope with phase contrast lens alignment (BX50; Olympus, Tokyo, Japan) equipped with the CCD camera (ORCA-HR C4742-95-12NR; Hamamatsu Photonics, Shizuoka, Japan) was used. Observation for charcoal particles was carried out with a differential interference contrast microscope (BX60; Olympus) a CCD camera (DP70; Olympus). For confocal laser scanning microscopy (CSLM) observation, LSM510 (Zeiss, Oberkochen, Germany) was used.

Results

Observation of glycocalyx

To examine dynamics of the glycocalyx during locomotion, cells stained with fluorescently labeled Alexa488 Con A were observed. To examine dynamics of the glycocalyx of *A. proteus*, especially eligibility of the RLF model, the cell surface of *A. proteus* pulse-stained with fluorescent labeled Alexa488 Con A for 0.3 h, and time-dependent change of the fluorescence signal after washing was observed with a fluorescence microscope. If membrane supply at the leading region during amoeboid locomotion of *A. proteus* is highly dependent on exocytosis from a large pool of internal membrane, such supply of the un-labeled cell surface will dilute the fluorescence signal at the leading region. However, peripheral fluorescence intensity did not change during locomotion (Fig. 5). Furthermore, the intracellular fluorescence signal was not detected up to 20 minutes from the staining. These observations are inconsistent with the RLF model.

Pinocytosis induction

Alexa 488 Con A fluorescence did not detect within the cell for 20 minute from the staining, but the punctate intracellular fluorescence signal gradually increased for 3 h (Figs. 6A and 6C). Although such internalization of the glycocalyx was only seen in the longer incubation, still it suggests that some amount of the cell surface endocytosed into the cell can be used to expand the leading edge of the locomoting amoeba. To estimate contribution of endocytosis and exocytosis to the amoeboid movement, I analyzed amoeba whose pinocytosis is activated by exposing egg albumin (Stockem and Korohoda 1975). As a result, the uptake of glycocalyx remarkably increased compared to untreated cells (Figs. 6B and 6D). However, locomotion activity of treated cells did not rise relative to untreated cells (data not shown). These results suggest that the slow uptake of the glycocalyx is caused by pinocytosis, but has minor, if any, contribution to amoeboid movement.

Cell surface movement

Because Alexa 488 Con A labels amoeba cells uniformly, it is useful to

monitor internalization and externalization of the glycoalk. On the other hand, it is unsuitable to visualize movement of a part of the glycocalyx during amoeboid motion. Next, I used charcoal particles to label particular parts of the glycoalk. Charcoal particles adhered in both anterior and posterior regions of amoeba cells moved forward in many cases (Fig. 7 - Fig. 10). In both of the regions, most charcoal particles on dorsal and lateral surfaces moved forward (Figs. 7 and 8) while those on the leading edges showed tendency to stay at the same positions of the cells (Figs. 9 and 10). I became aware that a few particles adhered at the rear side of retracting pseudopods stayed at the same positions against the glass slide for a while and even moved backward (Fig. 10F). All of the observed charcoal particles on the ventral surface stayed at the same positions against the slide (Fig. 11), but they might have attached to the substrate but not the cell surface. The above movement of cell surface portions monitored by charcoal labeling, especially that of the dorsal part, is consistent with the TFU model (see Fig. 3 and Discussion in detail)

Discussion

In this chapter, I analyzed dynamics of the cell surface during amoeboid movement of *A. proteus* using two different labeling techniques. First, I analyzed turnover of the glycocalyx by Alexa488 Con A staining to examine contribution of endocytosis and exocytosis to pseudopod formation. Fluorescence intensity at the leading edge of pseudopod did not change during amoeboid movement (Fig. 5). If the plasma membrane dynamics of *A. proteus* follows the RLF model, the fluorescence intensity at the edge must become lower gradually because of addition of plasma membrane at this part of the cells. Moreover, intracellular fluorescence signals were not detected up to 0.3 h after pulse-staining with Alexa 488 Con A by CSLM (Fig. 6A). These results strongly suggest that dynamics of the cell surface in *A. proteus* were not mainly governed by the RLF model, which requires active endocytosis and exocytosis for amoeboid movement.

On the other hand, uptake of the glycocalyx was detected in cells after a prolonged incubation (Fig. 6C). Considering migration velocity and cell size of *A. proteus*, the observed uptake of the glycocalyx seems to be insufficient for cell surface supply during cell movement. Uptake of the glycocalyx remarkably increased in the presence of a pinocytosis inducer, egg albumin, while locomotion of the amoeba cells was not activated, suggesting that there is no tight coupling between membrane dynamics driven by endocytosis/exocytosis and amoeboid locomotion. Because a part of the glycocalyx of *A. proteus* is continuously left on the substrate during movement, amoeba cells must perform endocytosis and exocytosis to replenish the cell surface with the new glycocalyx (Komnick, *et al.* 1973). Probably, the uptake of glycocalyx only work as a process for renewal of the glycocalyx.

Next, I inspected movement of each part of the cell surface using charcoal particles adhered on the surface of amoeba cells as markers. In the rolling motion model, the dorsal surface movement precedes that of the ventral surface, which stays at the same position against the substrate. In any experiments, charcoal particles on the dorsal surface moved forward, and the ventral surface did not, being consistent with prediction from the rolling motion model (Fig. 10 and 11). However, in the rolling motion model, the dorsal surface should move to the ventral surface when reaches the

anterior edge, and the ventral surface turns to the dorsal surface when arrived at the posterior edge. Most particles on the anterior and posterior edges stayed at the same positions (Fig. 7, 8), thus the plasma membrane dynamics of *A. proteus* is presumed to be differed from the rolling motion.

Both dorsal and ventral surfaces must stay in the same positions against the substrate in the RLF model, whereas charcoal particles in the dorsal surface of *A. proteus* moved forward in my experiments. These results are also against the RLF model. In the TFU model, both dorsal and ventral surfaces should move forward, and the cell surface should not move at the adhesion site and at the leading and retracting edges. The observed movement of charcoal particles on amoeba cells are almost consistent with these prediction drawn by the TFU model. However, the fact that particles on the ventral surface always stayed against the substrate, is not fit to the prediction by the TFU model. Griffin and Allen (1960) reported this motion, it is considered that particles in the ventral surface actually attached to the substrate or attached to the adhesion site.

In these circumstances, these results are against the rolling motion and RLF models. These mostly support the TFU model, whereas the result pertinent to the ventral surface does not conform with the prediction from the TFU model. To verify this conflict, the dynamics of the ventral surface is required to be observed by accurate microscopy. In next chapter, I introduced new microscopy for of the dynamics of the ventral surface..

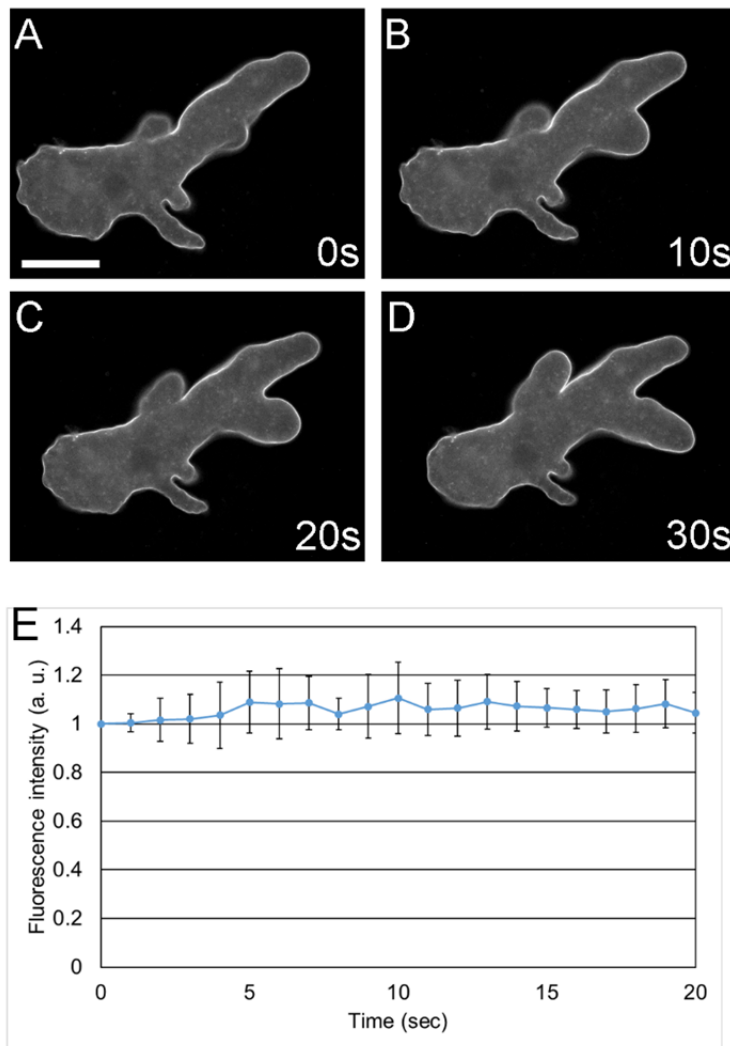


Fig. 5 Time-lapse image of *A. proteus* stained with Alexa 488 concanavalin A

(A-D) *A. proteus* was stained with Alexa 488 Con A is described in Materials and Methods. Observation was started at 5min after staining, and fluorescence image were taken at 0 s (A), 10 s (B), 20 s (C) and 30 s (D). Bar = 50 μ m. (E) Quantitative analysis of fluorescence intensity at the pseudopod edge. Each data point represents an average of 10 measurements with a standard deviation as an error bars.

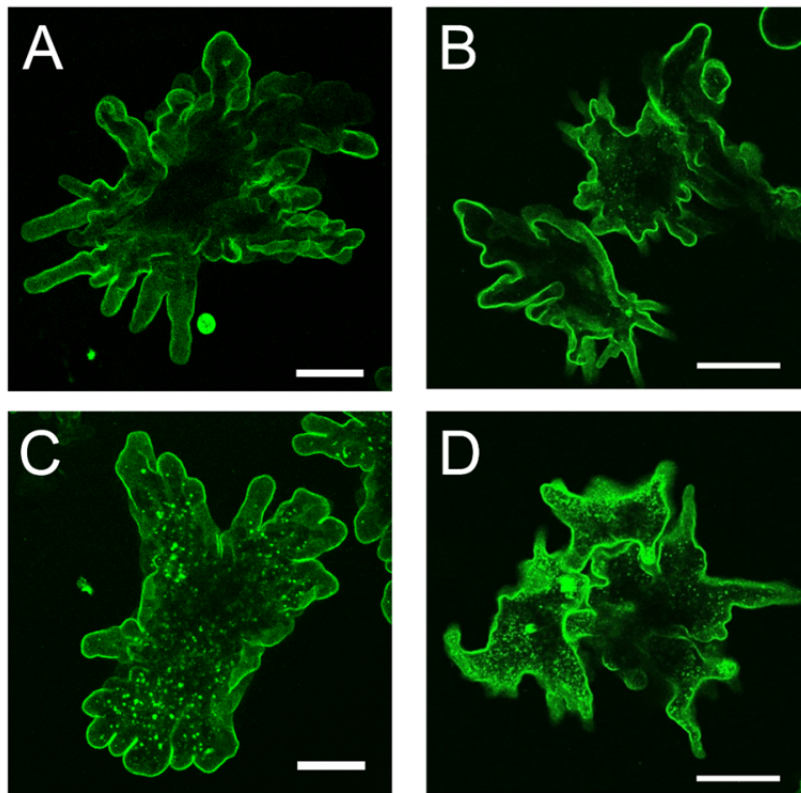


Fig. 6 Uptake of Con A fluorescence during a long incubation period.

(A-C) *A. proteus* cells were stained with Alexa 488 Con A as in Fig. 5, and the cells were observed under the microscope at 0.3 h (A), 1 h (B) and 3 h (C) after the wash. (D) Alexa 488 Con A-stained cells were incubated in the presence of 2 % (w/v) egg albumin for 1 h. Bar = 50 μ m (A, C), 100 μ m (B, D).

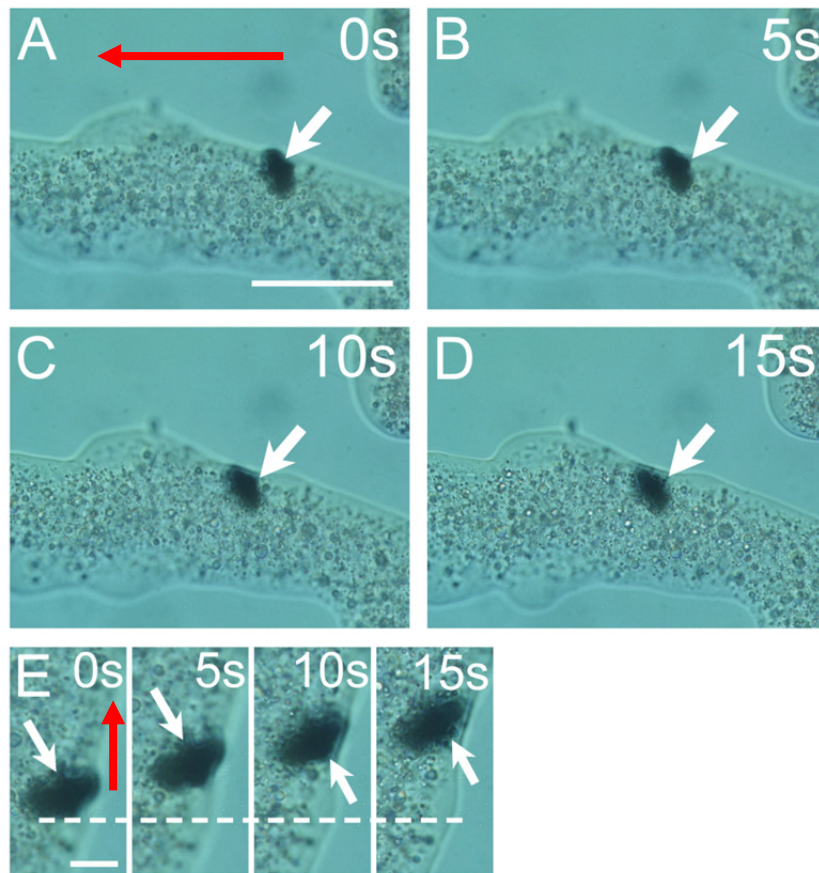


Fig. 7 Motion of a charcoal particle on the dorsal surface

(A-D) Time laps photographs of a charcoal particle adhered on the lateral side of a pseudopod. The amoeba cell was moving from the right to the left. (E) Higher magnification of the charcoal images. Red arrow, direction of amoeba movement; dashed line, the position of the charcoal particle at time 0. Bar = 50 μm (A), 10 μm (E).

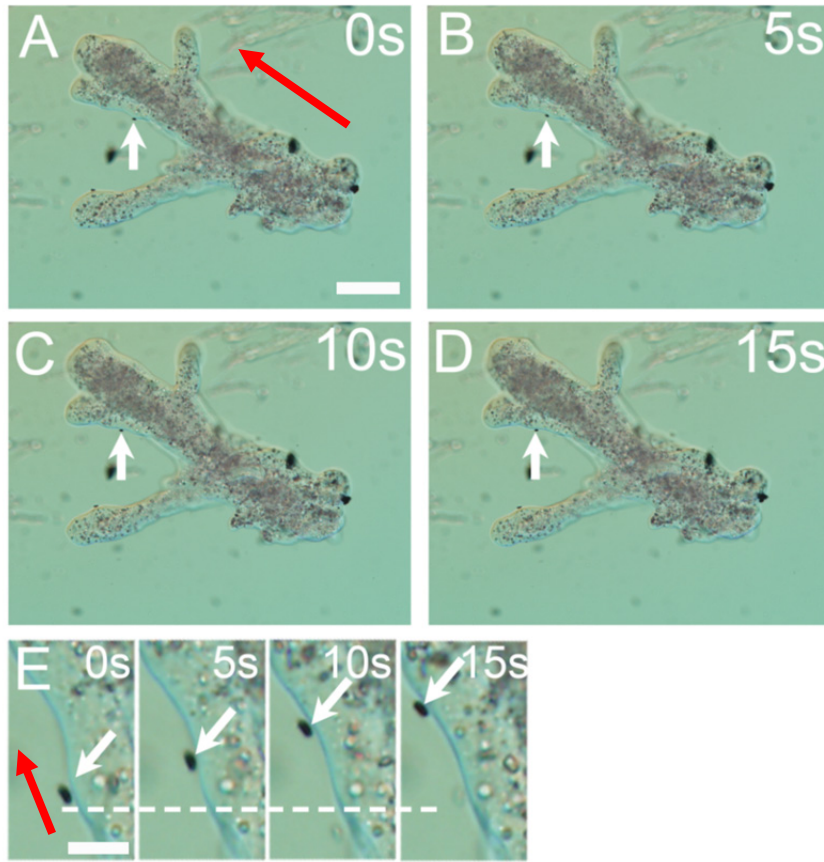


Fig. 8 Motion of a charcoal particle on the lateral side of a pseudopod

(A-D) Time laps photographs of a charcoal particle on moving amoeba. (E) Higher magnification photographs of a charcoal particle adhered on the lateral side of a pseudopod (marked with an arrow in panels (A-D)). All the images are presented essentially as Fig. 10. Red arrow, direction of amoeba movement; dashed line, the position of the charcoal particle at time 0. Bar = 50 μm (A), 10 μm (E).

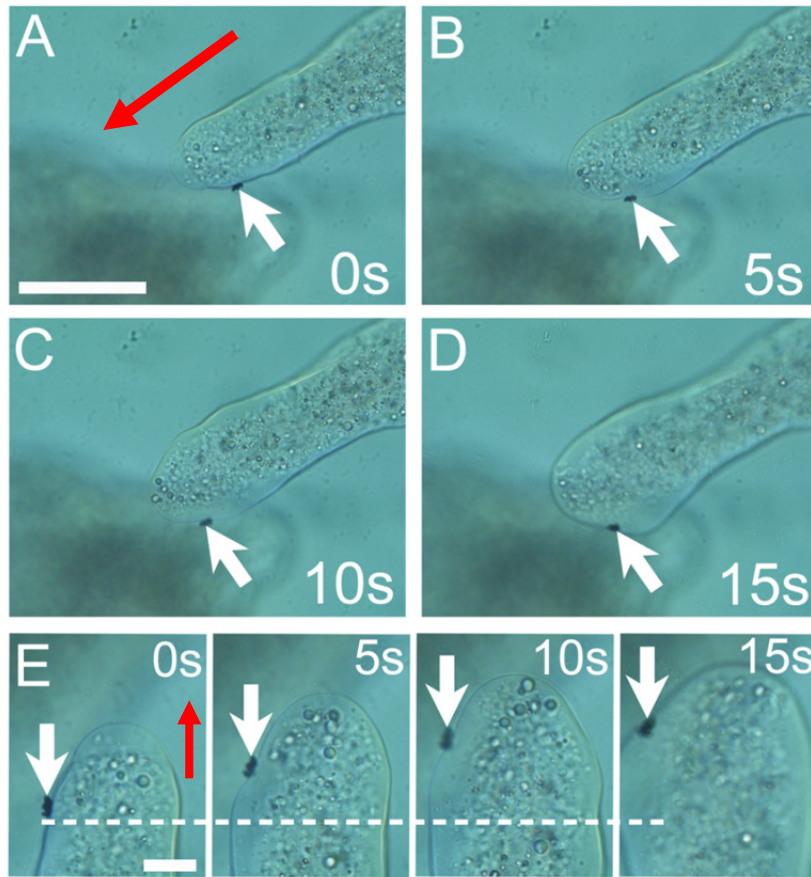


Fig. 9 Motion of a charcoal particle at the anterior edge of a moving amoeba

(A-D) Time laps photographs of a charcoal particle at the anterior edge. (E) Higher magnification images of (A-D). Only the leading edge portion of the amoeba is shown. Charcoal particle (arrow) migrated to the forward, but stayed at the anterior edge. Red arrow, direction of amoeba movement; dashed line, the position of the charcoal particle at time 0. Bar = 50 μm (A), 10 μm (E).

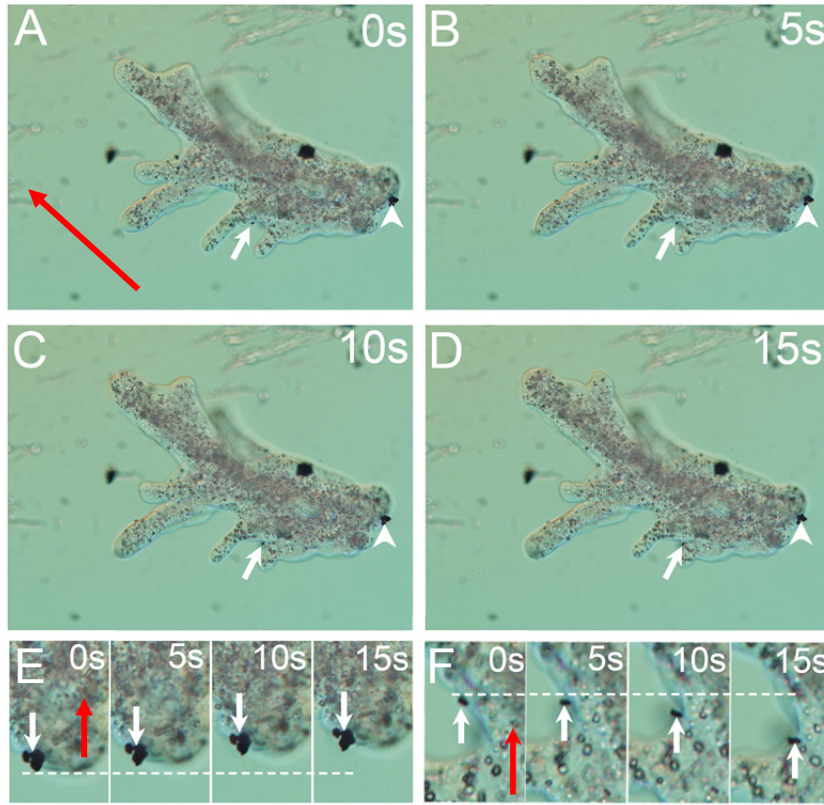


Fig. 10 Motion of charcoal particles on the posterior region of a moving amoeba

(A-D) Time laps photographs of charcoal particles adhered on the posterior region of *A. proteus*. Images were taken at every 5 s. The amoeba was moving in the direction indicated with a red arrow. (E) and (F) Parts of the images in (A-D) were shown at higher magnifications. A charcoal particle on the posterior edge marked with on arrowhead in panels (A-D) was shown in (E). Another particle on the rear of folds near a retracting pseudopod (marked with an arrow) was in (F). Dashed line, the position of the charcoal particle at time 0. Bar = 50 μm (A), 10 μm (E, F).

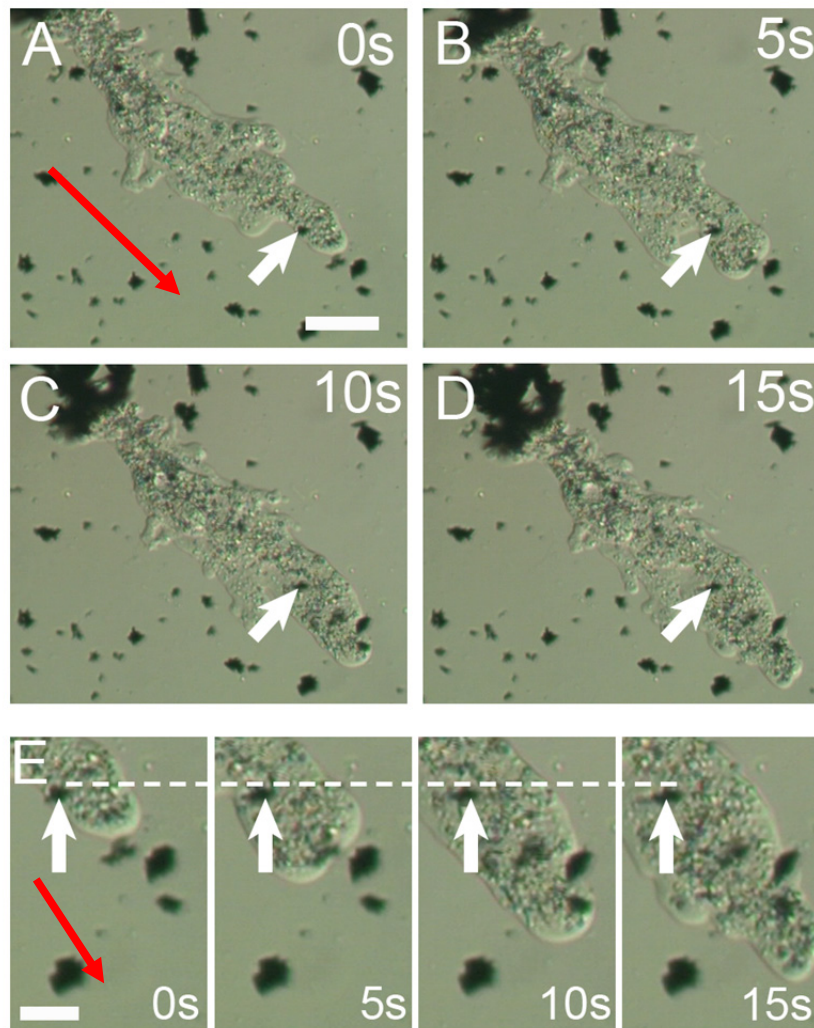


Fig. 11 Motion of a charcoal particle on the ventral surface of moving amoeba

(A-D) Time laps photographs of particles on moving amoeba. (E) Higher magnification photographs of a charcoal particle see in the ventral side (indicated by an arrow). Red arrow, direction of amoeba movement; dashed line, the position of the charcoal particle at time 0. Bar = 50 μm (A), 20 μm (E).

Chapter II

Dynamics of cell surface and cytoplasm

Abstract

To reveal the dynamics of the ventral plasma membrane of *A. proteus* a whole cell was observed as a section by Digital Scanned Light-sheet Microscopy. This observation allows monitor dynamics of the dorsal and ventral surface simultaneously in addition to the cytoplasm. To visualize the surface and interior of a cell, the cell surface was labeled with a fluorescent dye using dyes, 1,1'-dioctadecyl-3,3,3',3'-tetramethylindocarbocyanine (DiI), and mitochondria in the cytoplasm was stained with MitoTracker Deep Red. The ventral cell surface was found to move forward as the case of the dorsal side. In contrast, the cell surface of folds in the posterior region did not move. These observations suggest that the plasma membrane dynamics of *A. proteus* follows the TFU model. In addition, these results indicate that the glycocalyx of *A. proteus* has high plasticity. The mitochondria near the plasma membrane, of which movement exemplifies flow of the cytoplasm, rather stayed against the substrate while the cell surface near those mitochondria moved forward. This means that the plasma membrane slide on the cytoplasmic gel during amoeboid movement.

In the TFU model, the cell requires to adhere to the substrate through some parts of its ventral side. Indeed, such adhesion sites on the ventral side were observed with a spinning-disk confocal microscope, while the most of the ventral cell surface moved forward.

Dynamics of glycocalyx and cell surface were observed in the above experiments, but that of the plasma membrane was not examined. For this reason, dynamics of the glycocalyx and the plasma membrane was observed using the cells stained with Alexa488 Con A and detergent-solubilized DiI, which labeled the glycocalyx and the plasma membrane, respectively. Patterns of Alexa 488 Con A and DiI fluorescence signals introduced by photobleach exhibited almost the same movement along amoeboid locomotion. Therefore, these results suggest that the plasma membrane dynamics cooperates with the glycocalyx dynamics.

Introduction

In the previous chapter, I showed that the dorsal surface of *A. proteus* moves forward and the ventral surface stays against the substrate during amoeboid movement. Many other observations in the previous chapter support the TFU model for dynamics of the cell surface and are against the other two models, namely the rolling motion and RFL models. On the other hand, the static nature of the ventral surface observed by charcoal particle-labeling is not fit to the TFU model. Although another new model might be taken into account, the possibility that all the charcoal particles observed in the ventral surface are just attached to the substrate but not the amoeba cell can not be excluded. To clarify this problem, more precise cell surface labeling and a new observation technique that allow visualization of both dorsal and ventral sides of moving amoeba cells simultaneously are required. As a microscopic technique to fulfill such demands, there is specialized confocal microscope named Digital Scanned Light-sheet Microscope or DSLM.

DSLM was developed by Stelzer and colleague in European Molecular Biology Laboratory (Keller *et al.* 2008). In this system, a galvano mirror swings laser beam to form the light-sheet, which enables to scan in high-speed (Fig. 12). The fluorescent image is obtained by the scan corresponding to the line scan and can reduce bleach as compared with usual CLSM. In DSLM, the detection lens is set at a right angle to the excitation beam. Samples can be observed at a desired angle against the light path axis for detection (Fig. 13). If the support holding sample cells is set in parallel with the detection axis, both near and far sides against the support can be recorded in the single image.

Therefore, this technique is suitable to take optical sections of a moving amoeba cell in real time.

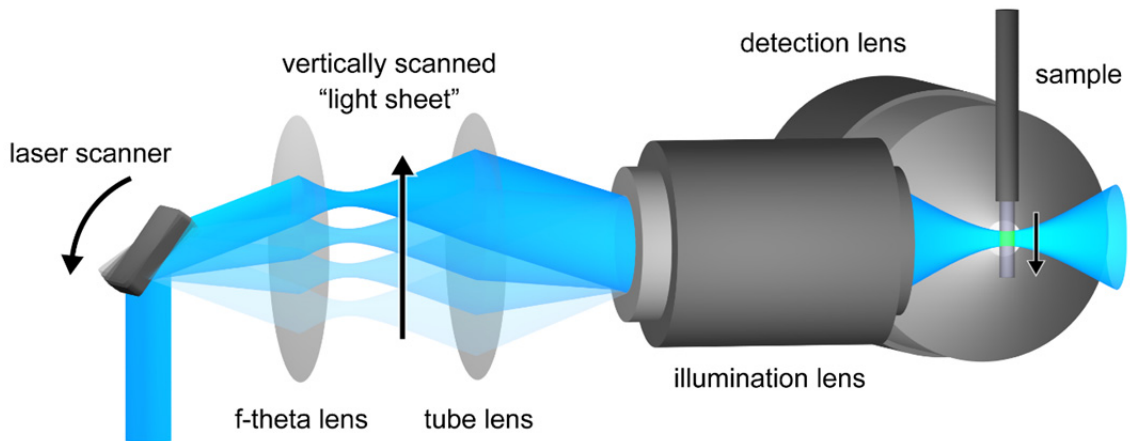


Fig. 12 Digital Scanned Light-sheet Microscopy (DSLM).

A schematic drawing of the light path of DSLM. Note that the illumination and detection axes are set at a right angle with each other. The sample is scanned in high-speed by light-sheet (from Keller *et al.* 2008).

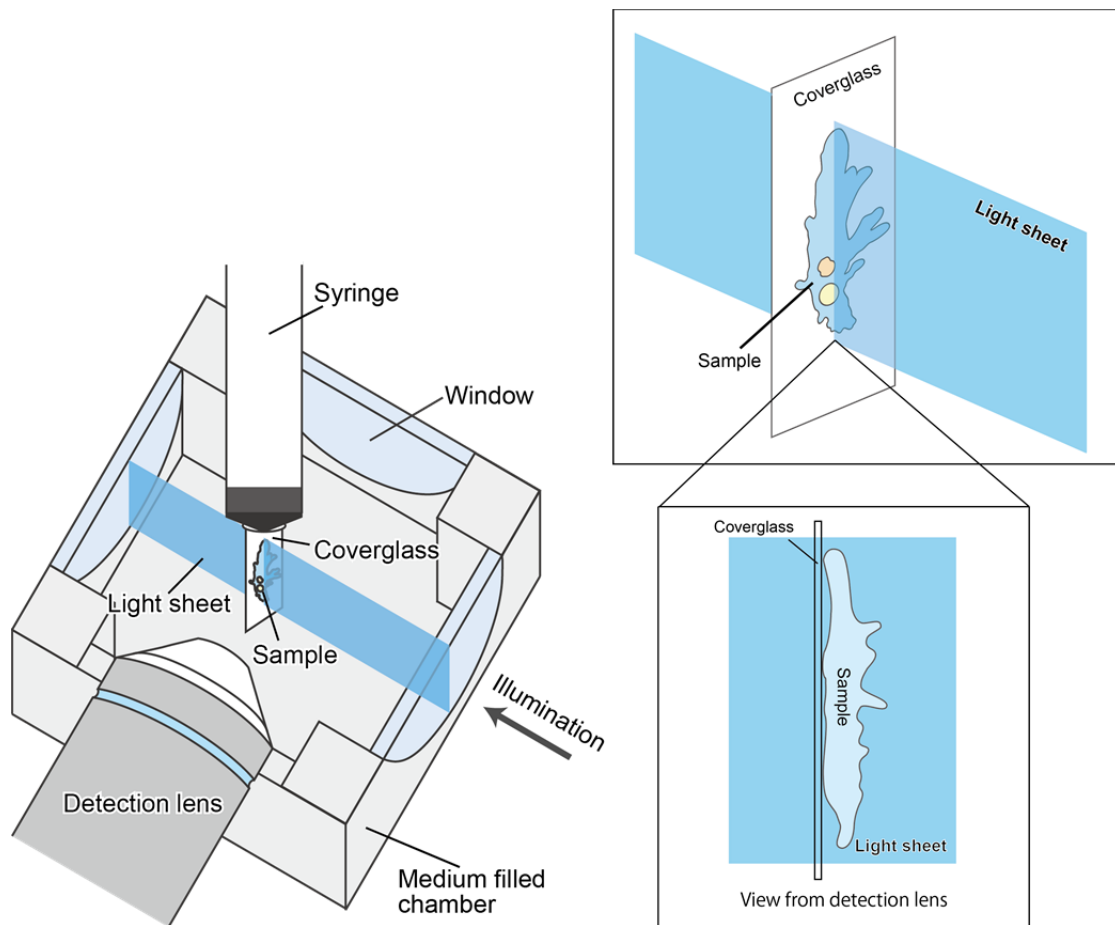


Fig. 13 A schematic view of the sample chamber of DSLM.

The sample chamber of DSLM is schematically illustrated. A coverslip with samples is set in the chamber in parallel with the detection axis to allow “sectioning” the samples by the light-sheet excitation

Materials and Methods

Cell culture

A. proteus was cultured in plastic boxes (30 x 22 x 5 cm) filled with the KCM medium (9.39 μ M KCl, 32.5 μ M $\text{MgSO}_4 \cdot 7\text{H}_2\text{O}$, 54.4 μ M $\text{CaCl}_2 \cdot 2\text{H}_2\text{O}$) at 25 °C, and feeded with *Tetrahymena pyriformis* twice a week. *T. pyriformis* was cultured 2 %(w/v) Bacto Proteose Peptone (Becton, Dickinson and Company) medium for three days. Cells were starved for at least three days before experiments.

Digital scanned light sheet microscopy (DSLM)

DSLM in National Institute for Basic Biology was based on European Molecular Biology Laboratory systems. DSLM equipped with Ar-Kr laser (35 LTL 835; Melles Griot, NM, USA), Plan-Apochromat lens with 5x magnification and 0.16 NA (Zeiss) is an illumination lens and a W Achroplan lens with 40x magnification and 0.80 NA (Zeiss) as a detection lens and a CCD camera (ORCA-AG; Hamamatsu) for detection.

Staining of the cell surface and mitochondria

The cell surface of *A. proteus* was stained with 2.68 μ M DiI (Invitrogen) for ten min., and the cells were washed three times with the fresh medium. The cells were also stained with 0.92 μ M MitoTracker Deep Red 633 (Invitrogen) for 5 min., and were washed three times with fresh medium.

Sample mount

To control locomoting direction of *A. proteus*, the cell extract of homogenized *T. pyriformis* was put on the cover slip with a syringe and dried. Subsequently, cells put on this cover slip and was mounted to with the DSLM chamber (Fig. 13).

Observation of the ventral glycocalyx

The glycocalyx of *A. proteus* was stained with 5 μ g/ml Alexa488 ConA

(Invitrogen) for five min., and the cells were washed three times with the fresh medium. Subsequently, cells were put in a chamber on a glass slide with an approximate thickness of 200 μm . Samples were observed with a spinning-disc confocal microscope from the ventral side of the amoeba cell solubilized-detergent. Spinning-disk confocal microscopy was performed with a inverted microscope (ECLIPSE Ti-E, Nikon, Tokyo, Japan) equipped with a spinning disk scanning unit (CSU-X1-M; Yokogawa Electric, Tokyo, Japan) and EM-CCD camera (iXonEM+ -DU897E-CSO-#BV; Andor Technology PLC, Belfast, Northern Ireland).

Observation of Plasma membrane and glycocalyx

To stain the plasma membrane of amoeba cells uniformly with DiI, 2.68 μM DiI solution in Pluronic F-127 (Pluronic F-127 20% solution in DMSO; Invitrogen) was first sonicated and mixed with a detergent to obtain final 2.68 μM DiI solution. *A. proteus* was stained with Alexa488 Con A as mentioned above, and then stained with solubilized-detergent DiI. Samples were observed by a CSLM. The cells stained with DiI and MitoTracker were mounted on a glass slide Vaseline (Wako, Osaka, Japan) to make a chamber and flattened by pressing the cover slip. Fluorescence derived from both DiI and Alexa 488 Con A in a defined part of the sample image. the cells was bleached by the laser illumination of CSLM (559 and 647 nm) for 3 min. For CSLM observation FV1000MPE (Olympus) was used.

Results and Discussion

Optical sectioning to observe the cell surface and the cytoplasm simultaneously with DSLM

In the past, the dynamics of ventral plasma membrane has not been observed extensively, because the markers (e.g. beads, charcoal particle) should attach to the substrate but not the ventral surface of the cell. In this study, I tried to analyze this ventral dynamics of the cell surface using the DSLM technique, which allows to observe optical sections perpendicular to the substrate with high scan speed. For visualization of the cell surface, I used DiI. Although DiI is a lipophilic fluorescent dye, which is used to label lipid bilayers, it forms small aggregates that label the glycocalyx of *A. proteus*, and its granular fluorescence signals can be used, like charcoal particles, to see movement of parts of the cell surface with higher resolution. Cytoplasmic flow was monitored by mitochondria movement, which was visualized with MitoTracker Deep Red. When moving amoeba cells were stained with these fluorescent probes and mounted on the DSLM set-up, I found that both ventral and dorsal cell surfaces moved forward and that the surface in the rear fold region did not move (Fig. 14). Especially, Fig. 14G represents detailed movement of a DiI cluster on the ventral surface of the amoeba cell. Although the images are turned 90 degree if compared with whole DSLM images of the moving amoeba cell in Figs 14A-14D, the DiI cluster (magenta) marked with a blue arrow clearly moved from the bottom to the top along the substrate (a large dark field in the left part of the images) while mitochondria (green) marked with a white arrow stayed at the same position in this time frame. Such forward motion in the ventral side is common in the moving amoeba cells (see Fig. 14I schematically summarizing movements of individual DiI clusters). These characteristics of surface movements in the dorsal side, the ventral side and the posterior folds of the locomoting amoeba are only explained by the TFU model but not by the rolling motion model or by the RLF model (Fig.1-Fig.3). Therefore, I conclude that the membrane dynamics of *A. proteus* during amoeboid locomotion is driven by folding of the cell surface in the posterior region and unfolding in the anterior region.

Next, I analyzed characteristics of cytoplasmic flow in different parts of an amoeba cell in detail, using movement of mitochondria as a marker.

The cytoplasm of an amoeba cell is divided into a gel part and a sol part. The plasma membrane is lined with the cytoplasmic gel as a mechanical support. Indeed, mitochondria near dorsal and ventral surfaces tended to stay at the same positions (Figs.14E~14H, white arrows). Because the cell surface near such cytoplasmic gel moved forward, there should be some slipping layer between the gel and the plasma membrane. On the other hand, cytoplasmic flow was observed in the central part of the cell, and mitochondria in the posterior region moved forward along with cell locomotion. It is to be noted that mitochondria in the central cytoplasmic flow moved faster than the DiI clusters on the dorsal and ventral surfaces (see the schematic view in Fig. 14I). These results suggest that the cell surface is pushed at the leading edge by the cytoplasmic flow, and this pushing leads sliding of the cell surface connected to the leading edge.

Parts of the ventral glycocalyx act as adhesion sites

The observation with DSLM supports the TFU model. However, cells must adhere to the substrate. The TFU model does not say anything about it. Prediction of ventral surface motion by the TFU model can be applied only average motion of this part of the cell surface, and the model is not inconsistent with existence of adhesion sites on the ventral surface. To search for specific ventral surface parts which *A. proteus* uses to adhere to the substrate, I stained living amoeba cells with Alexa 488 Con A, and observed the cell with a spinning disk confocal microscope from the ventral side. The most part of the ventral glycocalyx moved forward, but some parts of the ventral surface kept staying at the same positions against the substratum in the time frame of observation (Fig.15, highlighted with blue arrow heads in the panel D). These observations suggest that the cell surface of *A. proteus* is highly fluid, but in the ventral region of the cell, the cell surface is differentiated into two parts, one is fluid to allow the membrane supply to a new pseudopod, and the other is static to account for cell adhesion to the substrate.

Dynamics of Plasma membrane and glycocalyx

The cell surface of *A. proteus* consists of two layers, the glycocalyx and the plasma membrane. So far, I have traced movement of the cell surface

with probes that label oligosaccharides or the most outer part of the cell surface. Therefore, the above observations have revealed characteristics of the glycocalyx dynamics. Although the glycocalyx and the plasma membrane have tight relation in structure, it may be possible that these two entities move independently during amoeboid locomotion. To analyze dynamics of the glycocalyx and the plasma membrane simultaneously, these structures were labeled with different fluorescence probes: Alexa488 Con A for the glycocalyx and detergent-solubilized DiI for the plasma membrane. As shown above, DiI forms clusters in aqueous solution from its hydrophobic nature and can be only used to label the out-most part of the amoeba cell surface to give a punctate staining. However, if the suspension of DiI was sonicated and solubilized with a detergent, Pluronic F-127, the reagent gave uniform surface staining of amoeba cells (Figs. 16A and 16B). It will be reasonable to suppose that this uniform staining comes from labelling of the lipid bilayer of the plasma membrane through the hydrophobic nature of DiI. Then, using these stainings, I examined the dynamics of the glycocalyx and the plasma membrane at the same time. One problem of using Alexa 488-Con A and detergent-solubilized DiI is their uniform staining, which makes tracking of particular parts of the cell surface along time course difficult. To circumvent this problem, patterns of staining were introduced by photobleaching. DiI-Alexa488 Con A double stained amoeba cells were irradiated with strong laser beam to bleach a small region of their cell surface. Then, change and movement of the bleached area were monitored by real-time recording with a confocal microscope. Fig. 16 shows sequential photographs after photobleaching of *A. proteus* stained with Con A and DiI. Change of the shape of the bleached area corresponds movement of the cell surface according to amoeboid locomotion. Indeed, the bleached area became expanded in the upper left direction, which is consistent with membrane flow driven by pseudopod elongation in the same direction. As exemplified in the merged images, fluorescence signals from Alexa488 Con A and DiI were almost completely co-localized in the moving amoeba, except that some punctate DiI signals are so strong, if compare with Alexa488 Con A signals, that it is difficult to tell all the punctate signals are in the region stained with Alexa488 Con A. Anyway, most of the two signals coincide, so that the cell membrane and the glycocalyx move as one body during locomotion.

In this chapter, I successfully introduced the DSLM technique to

observe cell surface and cytoplasmic movement during amoeboid locomotion of *A. proteus*. Indeed, with the use of appropriate fluorescent probes, I could confirm over all forward movement of the dorsal and ventral side of the cell surface, the nearest and furthest sides, respectively, in the usual microscopic configurations. The light-sheet fluorescence microscope was originally developed to obtain optical sections of thick specimens, so that the sample mounting is quite unique to allow observation with the variable angle. This is one of the reasons that the DSLM enables concomitant observation of the dorsal and ventral sides of amoeba cells. On the other hand, for moving specimens like amoeba cells, it shows some difficulty to align the specimen against the illumination and observation axes with an appropriate angle. Despite this fact, the DSLM technique is a powerful tool to the analysis of amoeboid movement.

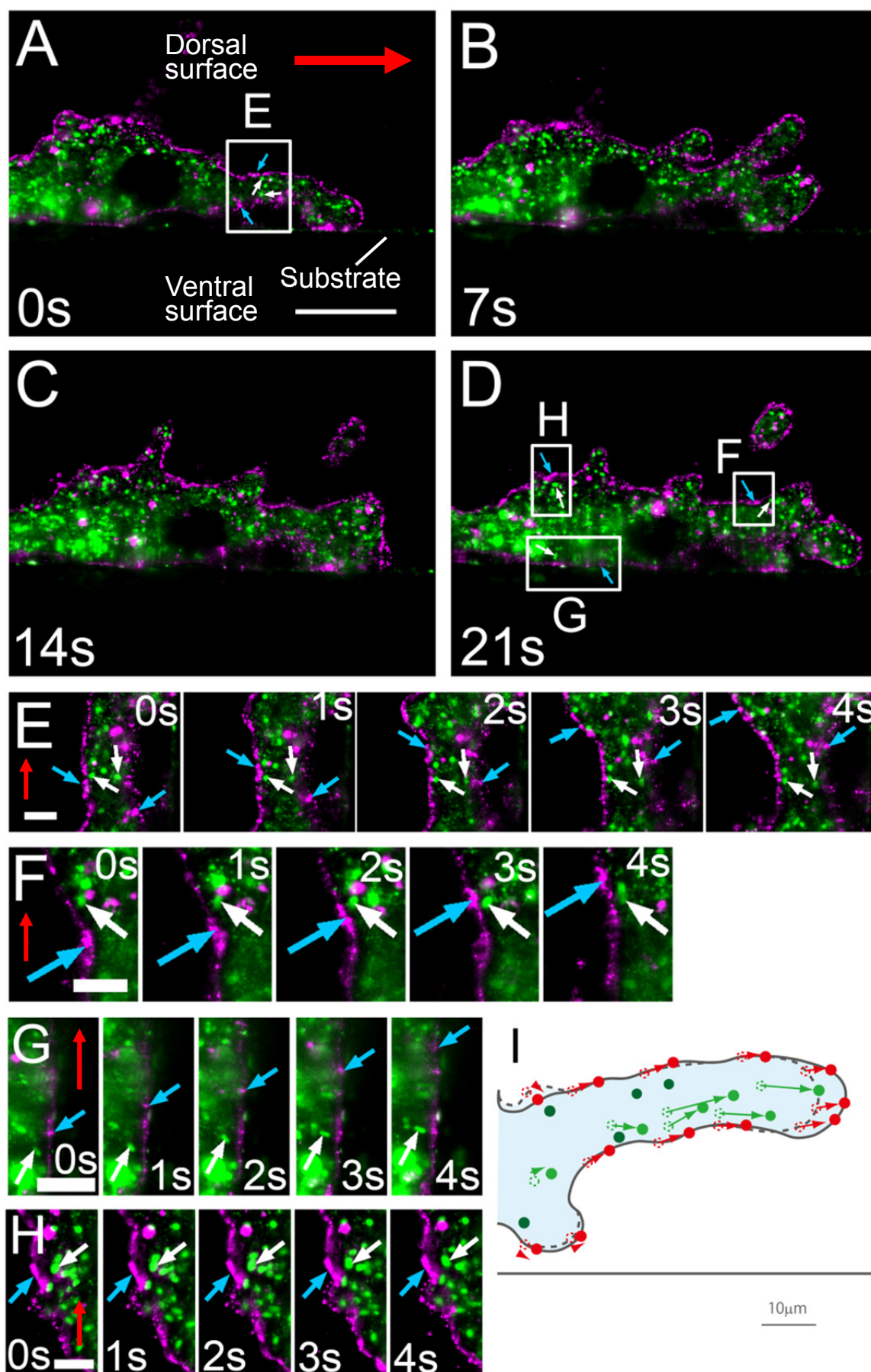


Fig. 14 Time-lapse analysis of optical sections of moving amoeba using the DSLM technique.

(A-D) *A. proteus* labeled with DiI (magenta) and MitoTracker (green). Observed by DSLM. (E-H) An area enclosed with rectangle E in the panel A, and rectangle F~H in panel D turned by 90 degree to the left (left, dorsal surface; right, ventral surface) and magnified. (E) DiI clusters (a blue arrow) on the dorsal and ventral surfaces in the pseudopod; (F) DiI clusters on the dorsal surface in the anterior region; (G) DiI clusters on the ventral surface in the anterior region; (H) DiI clusters on the rear of fold in the posterior region. A white arrow indicates mitochondria in the cytoplasmic gel. A red arrow indicates direction of amoeba movement. Bar = 50 μm (A), 10 μm (E-H). (I) Several DiI clusters and mitochondria in panel (A-D) were picked up and traced of these movement are schematically show.

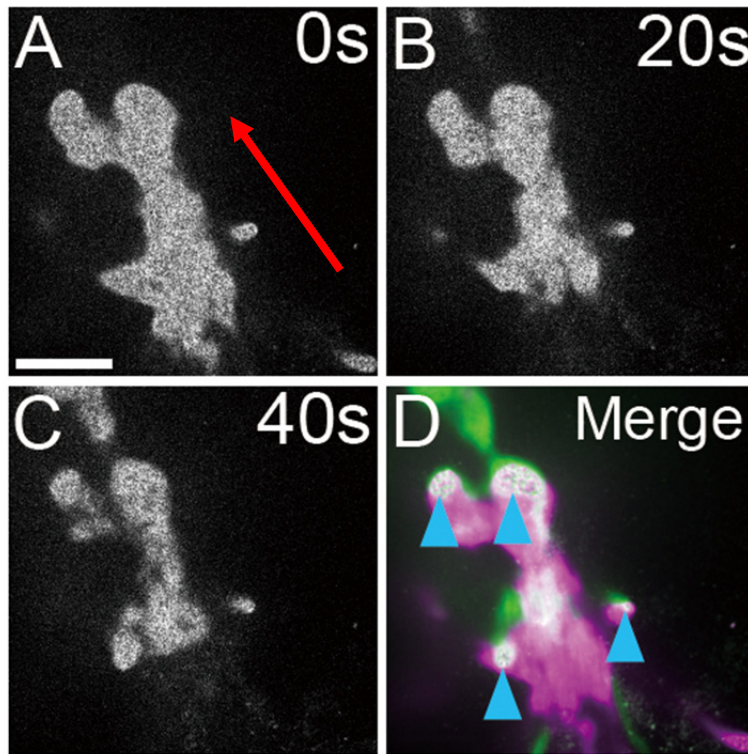


Fig. 15 Parts of the ventral glycocalyx are static against the substrate during amoeboid locomotion

(A-C) Time lapse photographs of *A. proteus*, stained with Alexa 488 ConA, obtained from the ventral side by spinning-disk confocal microscopy. (D) A composite image from sequenced photographs of A to 60 s (300 frames) (0→60sec: magenta→green) Arrow head, putative adhesion site; red arrow, direction of amoeba movement. Bar = 30 μ m.

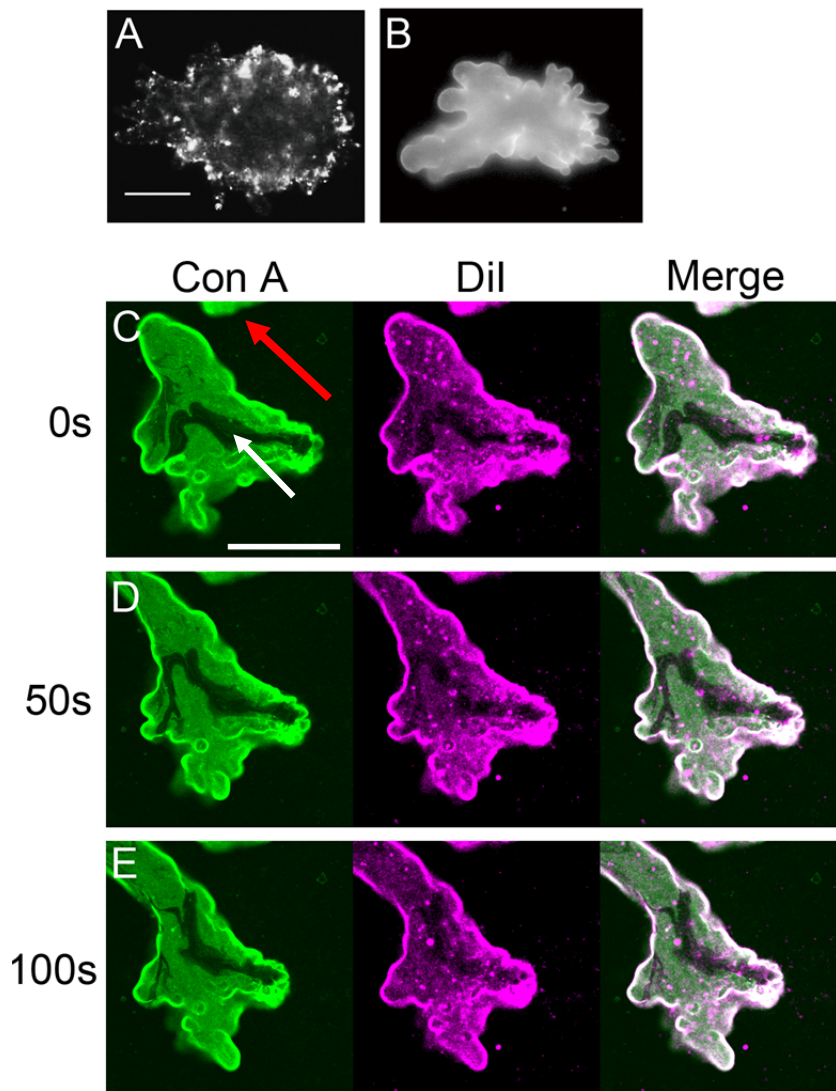


Fig. 16 Simultaneous observation of the glycocalyx and the plasma membrane

(A) Punctate staining with DiI suspended in water. (B) Uniform staining with DiI that was solubilized with pluronic F-127 and sonicated (C-E) *A. proteus* was stained with Alexa 488 Con A and DiI (in detergent), and photobleached by illumination laser of CLSM and then. Red arrow, direction of amoeba movement; white arrow, a bleach pattern. Bar = 100 μm .

Chapter III

Three-dimensional analysis of amoeboid movement

Abstract

To observe three dimensional movement of *Amoeba proteus*, I employed ezDSLM, an improved DSLM. In cells stained with DiI and MitoTracker, dorsal, ventral and lateral surfaces of cells moved forward in the extending pseudopod. The cell surface in the rear edge of folds did not move, but that moved forward in the posterior region of expanding folds. These observations further confirmed that *A. proteus* employs TFU model.

ezDSLM clarified cytoplasmic organization in the pseudopod. The cytoplasmic gel formed a tube structure and the cytoplasmic sol flowed in it. Mitochondria in the cytoplasmic gel did not move against substrate in extending pseudopod.

Rotation of the cell surface of a pseudopod at the uroid occurred, but did not mitochondria in the cytoplasm, indicating sliding between the plasma membrane and the cytoplasmic gel similar to the case described in Chapter II. I think this phenomenon might be induced by actin filaments associated with the plasma membrane and/or closely related to the physical property of the plasma membrane of *A. proteus*.

Introduction

In Chapter II, the cell surface and the cytoplasm of *A. proteus* were observed simultaneously as section using DSLM. In this observation, to keep the position, *A. proteus* was put on a guide line made by a cytoplasmic extract of *Tetrahymena*, but it was incomplete. Cells moved quickly to every direction, resulting in out-of-focus imaging. Moreover, it was difficult to analyze a rotating movement in detail, which was noticed in the previous study of Chapter II, by two dimensional observation using DSLM. To overcome such situations, three dimensional observation was thought to be ideal. DSLM could be applicable for three dimensional observation in some cases, but, a problem was in speed for obtaining images of *A. proteus*, which moves very quickly. If DSLM would be used in three dimensional observation, the sample holder must be shift more quickly, because detection lens is fixed to the sample chamber. However, the sample chamber was not designed to move at high speed. Spinning-disk confocal microscope was thought to be another candidate for 3-D observation. However, it requires to scan the whole of sample in the number of times, resulting in bleaching of fluorescence. ezDSLM has an advantage in avoiding bleaching of fluorescence by single scan. Moreover, in a spinning-disk confocal microscope, scattering light formed artifactual images derived from a pinhole disk because of high intensity of DiI clusters. Therefore, I decided to use ezDSLM, an improved DSLM, for three dimensional observation.

In ezDSLM, light-sheet is formed by the galvano mirror built-in CSLM and fluorescence is detected by the crosswise optical path. The sample chamber is designed to prevent samples from being exposed to vibration and detection lens is fixed to the chamber which is moved by a piezo linear stage with synchrony to scanning. Samples are fixed independent from the chamber. Thus, it becomes possible to obtain three dimensional images without vibration (Fig. 18).

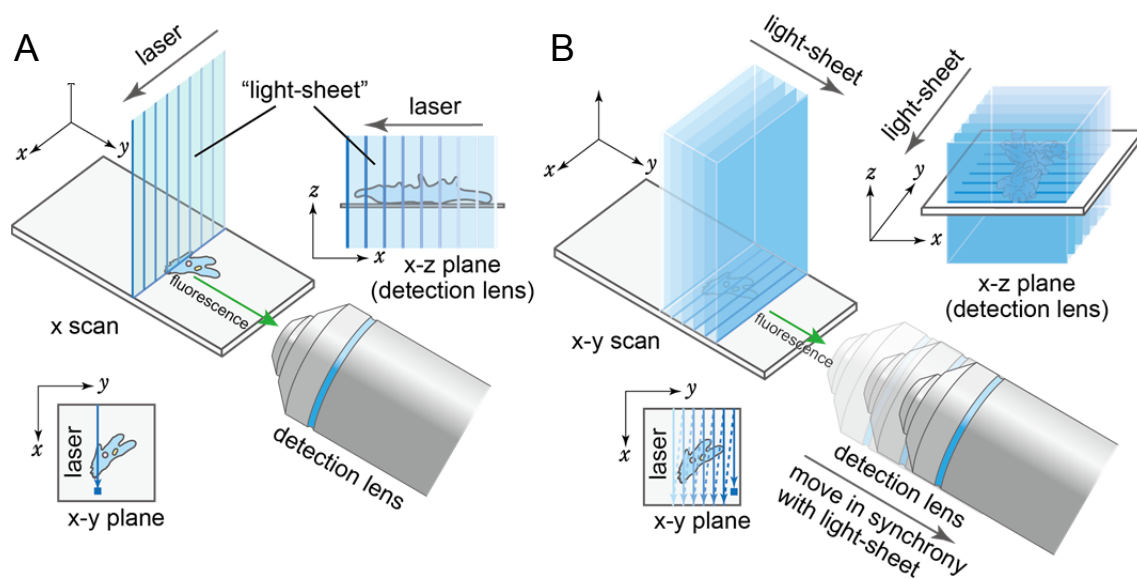


Fig. 17 Principle of ezDSL

(A) Line scan with makes an 'apparent' light-sheet similar to the conventional DSLM. (B) To obtain three-dimensional images, detection lens is moved in synchrony with light-sheet.

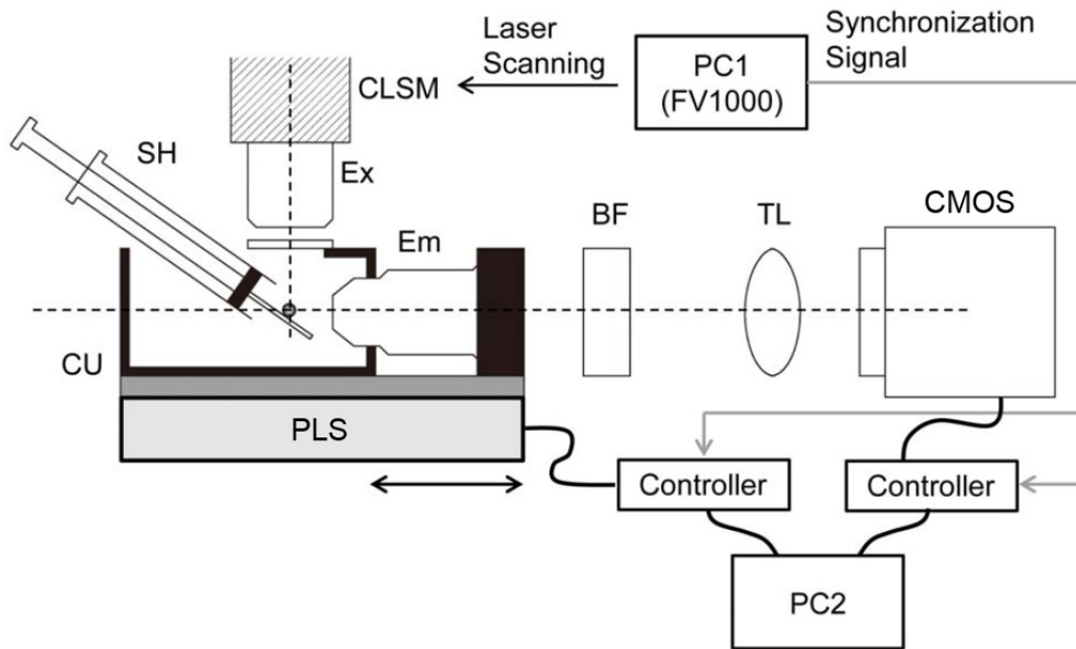


Fig. 18 Sample setting in ezDSLM

(A) Side view of the sample holder and the medium chamber to which detection lens (Em) is fixed (not to scale). Optical axes of objectives for excitation (Ex) and emission (Em) are shown in dashed lines. The illumination optics were derived from the confocal laser scanning microscope (CLSM). Specimens were placed on the sample holder (SH) in the chamber unit (CU) filled with medium. CU is mounted on a movable piezo linear stage (PLS). BF, barrier filter; TL, tube lens; CMOS, CMOS camera.

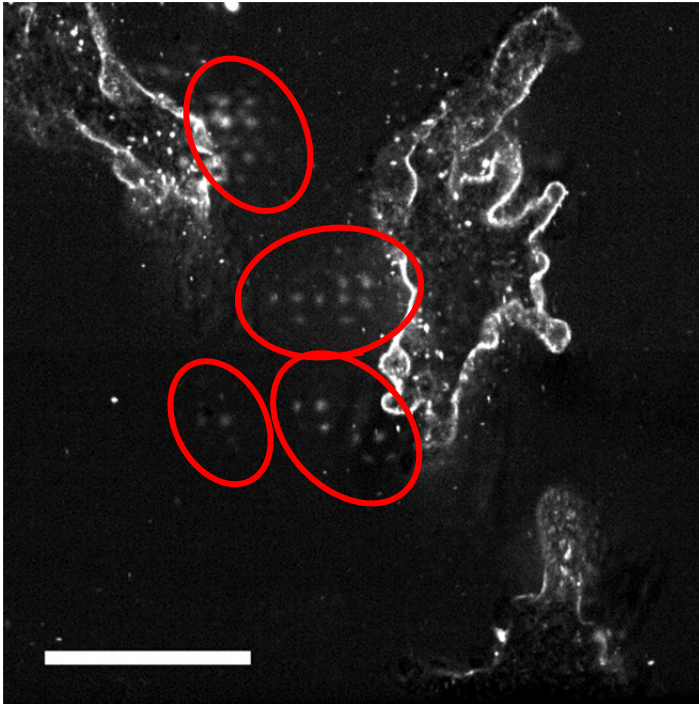


Fig. 19 Artifact appeared in spinning-disk confocal microscopy

A. proteus labeled with DiI. Observed with a spinning-disk confocal microscope. A red circle indicates pinhole disk pattern. Bar = 100 μm .

Materials and Methods

Cell culture

A. proteus was cultured in plastic boxes (30 x 22 x 5 cm) filled with the KCM medium (9.39 μ M KCl, 32.5 μ M MgSO₄·7H₂O, 54.4 μ M CaCl₂·2H₂O) at 25 °C, and fed with *Tetrahymena pyriformis* twice a week. *T. pyriformis* was cultured 2 %(w/v) Bacto Proteose Peptone (Becton, Dickinson and Company) medium for three days. Cells were starved for at least three days before experiments.

Staining of cell surface and mitochondria

Cell surface of *A. proteus* was stained with 2.68 μ M DiI (Invitrogen) for 10 min., and cells were washed three times with the fresh medium, and they were then stained with 0.92 μ M MitoTracker Deep Red 633 (Invitrogen, USA) for 5 minutes, and washed three times with fresh filled medium. Cells put on a cover slip and was mounted to the chamber unit filled with KCM medium.

Setup of ezDSLM

Setup of ezDSLM is schematically shown in Fig. 18. The FV1000 (Olympus) was used as the illumination optics. Excitation wave lengths were 559 and 647 nm, and the barrier filter (BLP01-561R-25 and BLP01-561R-25; Semrock, IL, USA) were selected for detection of DiI and MitoTracker Deep Red. The piezo linear stage (P-625.1CL; PI, Germany) and the piezo amplifier / servo Controller (E-665.SR; Physik Instrumente, Karlsruhe, Germany) were used for moving chamber unit. The stepsize of the stage was minimal incremental motion, 1.4 nm, and the moving range was up to 500 μ m. The movement of the stage was controlled by the original macros on the software, Mikromove (Physik Instrumente). The CMOS camera (ORCA-Flash4.0; Hamamatsu) was used for image acquisition. The camera was controlled by the HC Image software (Hamamatsu). The controllers were connected to a computer that is distinct from that in the FV1000 system. All electric devices were connected through their I/O interfaces, and the FV1000 system was used as a master of synchronization signals. Parameters for laser scanning (laser power, scan rate, spatial interval, *etc.*)

were controlled by the computer in the FV1000 system. The parameters were adjusted for imaging conditions, e.g., the increments and the range of movements for the light-sheet were typically 2.48 μm and 0.3 mm, respectively. When the FV1000 starts scanning, it outputs synchronization signals that are active during each line scan (“line active” signal). Exposures of CMOS camera were synchronized to the line active signals so that each line scan makes apparent light-sheet. The motion of the piezo linear stage was triggered by the line active signal and it moved at the constant rate that was synchronized to the movement of light-sheet. Trial-and-error processes may be required to adjust parameters at first, which can be achieved by imaging fluorescent microbeads or reflection of the glass surface as in the case of conventional light-sheet microscopy.

Results and Discussion

I developed ezDSLM, which I used to capture remarkably clear images of moving amoebae. This process did not require the specimen to be shaken because the light-sheet is optically scanned to obtain three-dimensional images. I demonstrated the clarity and speed of ezDSLM to outline the movements of *A. proteus*. The ezDSLM substantially extended the application of light-sheet based microscopy in biological field. Finally, since our system uses a conventional CLSM system for illumination optics, setup is very simple and easily adaptable to other laboratories.

DiI clusters attached to the pseudopod surface moved forward in every portions, dorsal, lateral and ventral surfaces. The clusters did not really move against the substrate in the rear of folds, while they moved forward in the region of expanding folds. Clusters attached to the posterior edge moved along with cell locomotion (Fig. 19). These observations were consistent with those in the previous studies (Chapter II) and confirmed that *A. proteus* employs the TFU model.

Because distribution and movement of mitochondria were clearly observed by ezDSLM, cytoplasmic architecture in the pseudopod became clear. Mitochondria adjacent to the plasma membrane did not flow, but those in the deep region flowed, indicating that the cytoplasmic gel formed a tube structure even in the thin pseudopod and the cytoplasmic sol flowed in it (Fig. 20).

In the posterior region, fluorescent spots of DiI occasionally rotated perpendicular to the axis on the surface of thin pseudopod like as a screwdriver (Fig. 21). The direction of rotation was varied. Rotation was observed in both attached and unattached pseudopod to the substrate and never observed in the large pseudopod in the anterior region. Mitochondria did not rotate, indicating again sliding between the plasma membrane and the cytoplasmic gel as in the case of the cell body. Rotation seemed to occur more frequently in a pseudopod just after detachment. This suggests that the pseudopod might have a twist strain during attachment to the substrate. Considering the fluidity of the plasma membrane, however, it is unlikely that such strain is given directly to the plasma membrane. If plasma membrane become rigid like as that in the adhesion site, it is possible. In this context, comparing organization of actin filaments under the plasma

membrane in both region is quite important because the fluidity of the plasma membrane could be regulated by actin. Alternatively, the plasma membrane which has glycocalyx might have a unique physical property that we have not known yet. It has been known that isolated plasmalemma take a rolling-up configuration like as a cigar. This configuration might be closely related to the rotation of the surface of pseudopod. Recently, Nishigami found a 28 kD polypeptide in the isolated plasma membrane fraction and preliminary experiments suggested the presence of this polypeptide in the amorphous layer. It is possible that the 28 kDa polypeptide might give a unique property to the cell surfaced *A. proteus*.

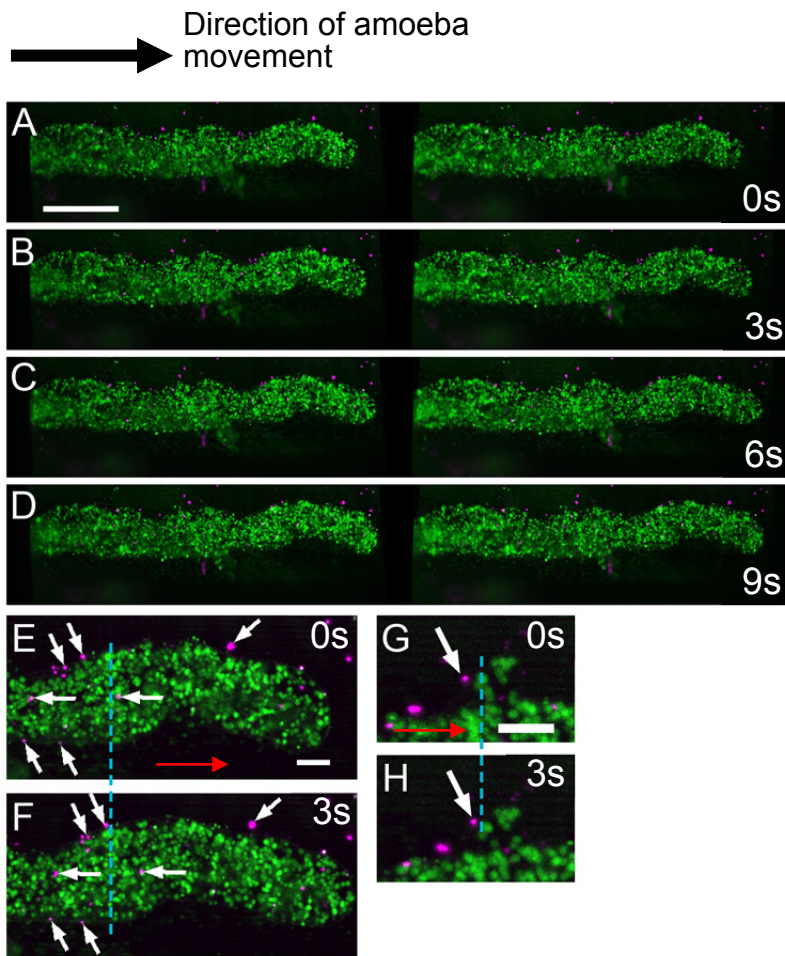


Fig. 20 Three-dimensional images of the cell surface and cytoplasm

(A-D) Stereo photographs of *A. proteus* labeled with DiI (magenta) and MitoTracker (green). obtained with an ezDSLM. (E) is high magnification of the pseudopod in the (A-D). (F) is high magnification of the fold in the (A-D). White arrows, DiI clusters; red arrow, direction of amoeba movement; blue dashed line, the reference line. Bar = 50 μm (A), 10 μm (E, F).

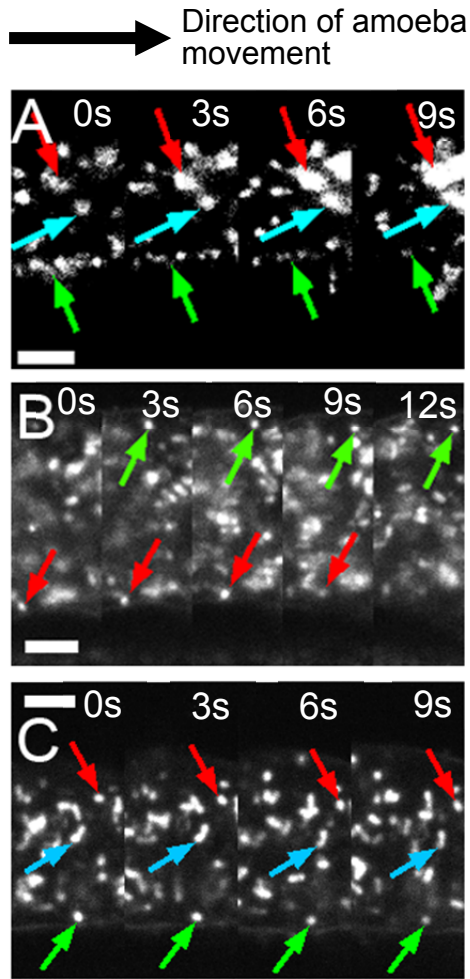


Fig. 21 Optical sections of the cytoplasmic gel in the pseudopod

(A-C) *A. proteus* labeled with DiI (not shown) and MitoTracker. Observed with an ezDSLM. As sequence of photographs of mitochondria in the far side of the pseudopod (A), optical section (B) and near side (C) to the detection lens. Arrows indicate mitochondria in the cytoplasmic gel. Bar = 10 μm.

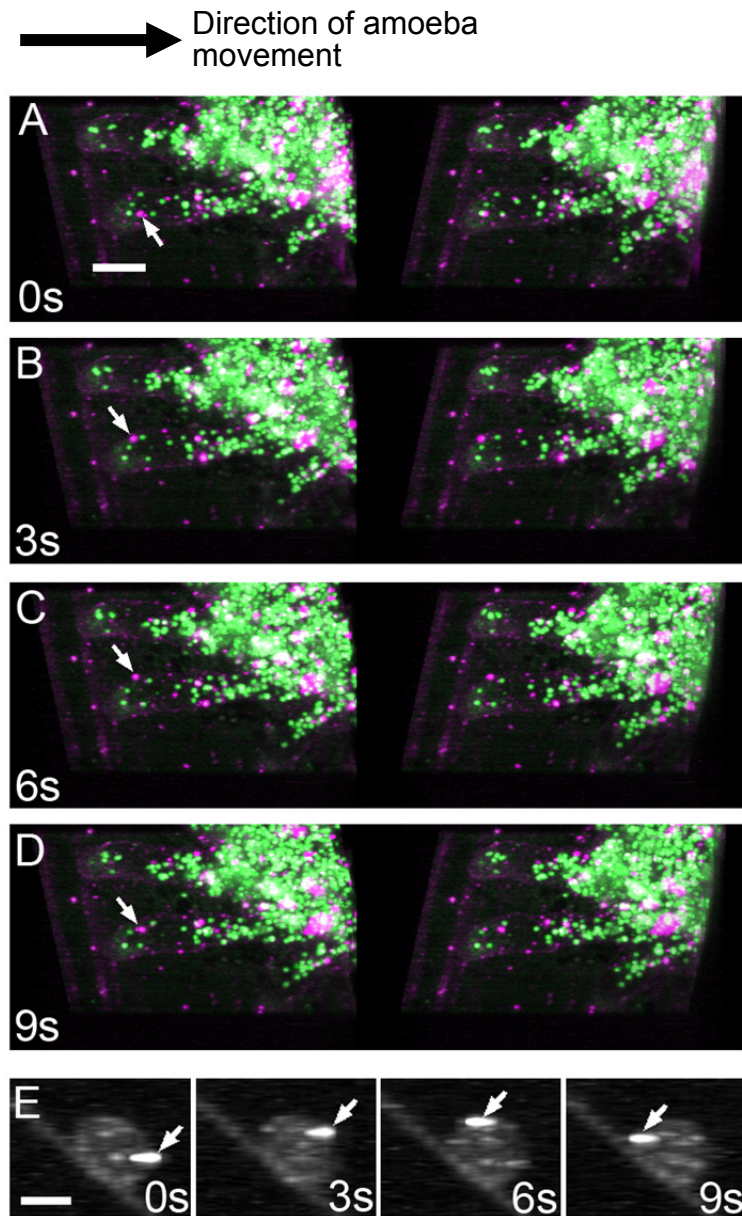


Fig. 22 Rotation of cell surface in the uroid

(A-D) Stereo photographs of *A. proteus* labeled with DiI (magenta) and MitoTracker (green), obtained with an ezDSLM. (E) shows optical sections of the uroid in (A-D). A white arrow indicates a rotating DiI cluster. Bar = 20 μm (A), 10 μm (E).

General Discussion

Understanding the movement of the plasma membrane is indispensable for understanding the mechanism of cellular locomotion of a wide variety of cells which show amoeboid movement, but not so much studies have been carried out. In this study, I have investigated the dynamics of the cell membrane (plasma membrane) of a free living giant amoeba, *Amoeba proteus* using improved optics and techniques. Studies by DSLM and ezDSLM techniques demonstrated that *Amoeba proteus* uses folds of the plasma membrane for extending pseudopod, predicted as the TFU model. Some previous reports proposed the RLF model for *A. proteus* based on electron microscopic observations. However, I could exclude this possibility by analysis of dynamics and direct observation of dynamics of the plasma membrane. In the same way, I could exclude the rolling motion model. However, I do not think that TFU model can completely explain the dynamics of the plasma membrane of *A. proteus*. For example, how the fluidity of the plasma membrane takes part in the dynamics. To answer this question, the organization and the function of actin filaments associated to the plasma membrane should be elucidated.

These actin filaments must be involved in cell attachment to the substrate, which is another interesting problem to be solved in future. *A. proteus* must perform cycling of attachment to and detachment from the substrate for locomotion. How *A. proteus* achieves this performance is not known. It is reasonable that actin filaments under the plasma membrane might play an important role in this process.

Another problem which cannot be explained by the TFU model is membrane rotation. This phenomenon was clearly demonstrated by the ezDSLM analysis. Considering the fluidity of the plasma membrane shown in the ventral surface, it is difficult to explain by the TFU model, because it is impossible to suppose any force that can induce deformation of such fluid-like structure. However, if the rigidity of the plasma membrane is regulated as described in Chapter III, I will get a clue to solve this problem.

If *A. proteus* simply uses membrane folds for extending pseudopod, the total area of the plasma membrane must be constant. I tried to estimate it using CLSM, DSLM and ezDSLM techniques, but I could not obtain complete 3-D image of *A. proteus*, because the images far from illumination

lens became hazey I suppose that this situation may be due to crystals contained abundantly in the cytoplasm, which scattered illumination light. To overcome this, I have a plan to improve ezDSLM which has two detection lens in opposite sides.

The cell surface moves forward but does not the cytoplasmic gel during locomotion of *A. proteus*. This was confirmed by using charcoal particle, DiI and MitoTracker and strongly suggested sliding between the plasma membrane and the cytoplasmic gel. Until now, people have realized that actin filaments in the cytoplasmic gel are linked to those associated with the plasma membrane, and that therefore the plasma membrane cannot slide on the cytoplasmic gel. Harberrey (1972) reported this phenomenon but did not discuss in relation to actin filaments included in the plasma membrane and the cytoplasmic gel. It is surprising that no one has noticed this relationship despite of many observations of *A. proteus* is decorated with marker substances. In addition, I could confirm the finding by Bovee (1970) that the sol layer is present between the plasma membrane and the cytoplasmic gel. (Fig. 23). This may be another indirect proof for the occurrence of the sliding. The presence of the cortical sol layer could be predicted by gel-sol conversion theory presented by Nishigami (2013), because shear stress should be generated between the plasma membrane and the cytoplasmic gel, if the sliding occurs. Of course, a possibility that the sol layer always exists between the plasma membrane and the cytoplasmic gel cannot be excluded.

Although sliding between the plasma membrane and the cytoplasmic gel was strongly suggested in my works, there remains a problem to be solved. If the lipid bilayer and the glycocalyx move independently, I have to basically reconstruct my theory on amoeboid movement. Photobleaching experiment indicated that both elements move as one body. However, I have no proof that DiI did stain the lipid bilayer. To elucidate this problem, I have to carry out additional experiment. For example, the use of more specific probe to the lipid bilayer or a GFP-conjugated membrane protein expressed in *A. proteus* instead of DiI may be possible, although no such probe or protein is known so far.

Finally, I would like to describe the mechanism underlying the amoeboid movement based on mainly the dynamics of the plasma membrane (Fig.24).

1. Calcium ion influx induces actin filament detachment from the plasma membrane and makes the cortical gel layer fragile.
2. The cytoplasmic sol effuses and pushes the plasma membrane.
3. The plasma membrane continue to be pushed and extends accompanied by expanding the folds.
4. At the same time, sliding between the plasma membrane and the cytoplasmic gel occurs and produces the sol layer

Appendix

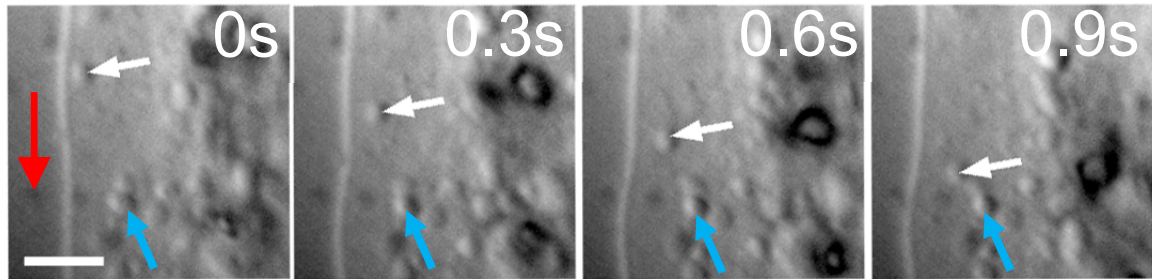


Fig. 23 Cytoplasmic sol in between the cytoplasmic gel and the plasma membrane

Time laps photographs of the adjacent plasma membrane on moving amoeba. (E) Red arrow, direction of amoeba movement; white arrow, the cytoplasmic sol between the plasma membrane and the cytoplasmic gel; blue arrow, the cytoplasmic gel. Bar = 5 μm ..

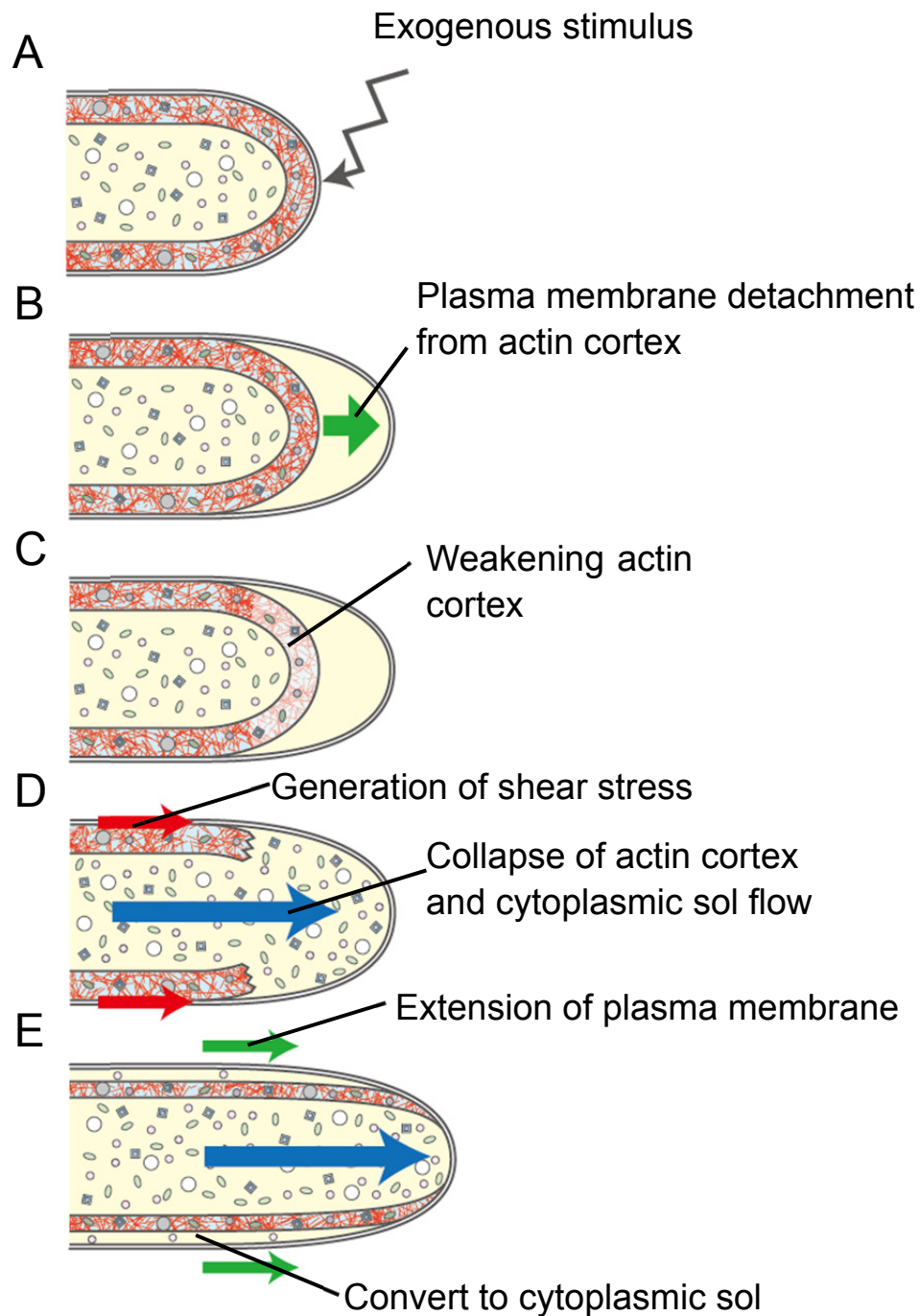


Fig. 24 Elongation of a pseudopod in *A. proteus*

A schematic illustration shows the process of pseudopod formation. (A) Calcium ion is increased by the exogenous stimulus. (B) The plasma membrane detach from actin cortex (C) The of actin cortex weakens (D) The tip of plasma membrane is pushed by cytoplasmic sol, the shear is generated stress generate between the plasma membrane and the cytoplasmic gel.

(E) The cytoplasmic gel is converted to the sol beneath the plasma membrane by the shear stress. The pseudopod extends by use of the plasma membrane of folds.

References

Abé, T. H.

Morpho-physiological Study of Ameboid Movement II. Ameboid movement and the organization pattern in a striata ameba.

Cytologia **27**, 111-139 (1962)

Allen, R. D.

A new theory of amoeboid movement and protoplasmic streaming.

Exp. Cell Res. **8**, 17-31 (1961)

Bell, L. G.

Surface extension as the mechanism of cellular movement and cell division.

J. Theor. Biol. **1**, 104-106 (1961)

Charras, G. T., Yarrow, J. C., Horton, M. A.,

Mahadevan, L., and Mitchison, T. J.

Nonequilibrium of hydrostatic pressure in blebbing cells.

Nature **435**, 365–369 (2005)

Charras, G. and Paluch, E.

Blebs lead the way: how to migrate without lamellipodia.

Nat. Rev. Mol. Cell Biol. **9**, 730-6 (2008)

Czarska, L. and Grebecki, A..

Membrane folding and plasma-membrane ratio in the movement and shape transformation in *Amoeba proteus*.

Acta Protozool. **4**, 201-239 (1966)

Fackler, O. T. and Grosse, R.

Cell motility through cell membrane blebbing.

J. Cell Biol. **16**, 879-84 (2008)

Goldacre, R. J.

The role of the cell membrane in the locomotion of amoebae, and the source of the motive force and its control by feedback.

Exp. Cell Res. Suppl. **8**, 1-16 (1961)

Goldacre, R. J.

On the mechanism and control of amoeboid movement. *In Primitive Motile Systems in Cell Biology*. Eds. By Alle, R. D., and Kamiya, N.,

Acad. Press, New York and London, 237-255 (1964)

Griffin, J. L. and Allen, R. D.

The movement of particles attached to the surface of amoebae in relation to current theories of amoeboid movement.

Exp. Cell Res. **20**, 619-622 (1960).

Haberey, M., Wohlfarth-Bottermann, K. E., Stockem, W.

Pinocytosis and locomotion of amoebae VI. Kinematographic studies on the behaviour of the cell surface of moving *Amoeba proteus*.

Cytobiologie **1**, 70-84 (1969).

Harberey, M. Reviewed

Cell Motility: Mechanisms in protoplasmic streaming and amoeboid Movement

Int. Rev. Cytol. **34**, 169-249 (1972).

Hausmann E. and Stockem W.

Pinocytosis and locomotion in amoebae. VIII. Endocytosis and intracellular digestion in *Hyalodiscus simplex*.

Cytobiologie, **5**, 282-300. (1972)

Hülsmann, N. Reviewed

Cell Motility: Mechanisms in protoplasmic streaming and amoeboid Movement

Int. Rev. Cytol. **34**, 169-249 (1973).

Jahn, T. L. and Bovee, E. C.

Protoplasmic movements within cells.

Physiol Rev. **49**, 793-862 (1969).

Kawakatsu, T., Kikushi, A., Shimmen, T. and Sonobe, S.

Interaction of actin filaments with the plasma membrane in *Amoeba proteus*: studies using a cell model and isolated plasma membrane.

Cell Struct. Funct. **25**, 269-277 (2000)

Keller, P. J., Schmidt, A. D., Wittbrodt, J. and Stelzer, E. H.

Reconstruction of zebrafish early embryonic development by scanned light sheet microscopy.

Science **322**, 1065-1069 (2008)

Komnick, H., Stockem, W. and Wohlfarth-Bottermann, K. E.

Cell Motility: Mechanisms in Protoplasmic Streaming and Ameboid Movement.

Int. Rev. Cytol. **34**, 169-249 (1973).

Lämmermann, T. and Sixt, M.

Mechanical modes of 'amoeboid' cell migration.

Curr. Opin. Cell Biol. **21**, 636-644 (2009).

Ley, K., Laudanna, C., Cybulsky, M. I. and Nourshargh, S.

Getting to the site of inflammation: the leukocyte adhesion cascade updated.

Nat. Rev. Immunol. **7**, 678-89. (2007)

Mast, S. O.

Structure, movement, locomotion, and stimulation in amoeba.

J. Morphol. **41**, 347-425 (1926)

Nishigami, Y., Ichikawa, M., Kazama, T., Ito, K., Kobayashi, R., Shimmen, T., Yoshikawa, K., and Sonobe, S.

Reconstruction of active regular motion in amoeba extract: Dynamic cooperation between sol and gel states.

PLoS ONE e70317 (2013)

Opas, M.

Course of glycerination of *Amoeba proteus*
and contraction of glycerinated models.

Acta Protozool. **15**, 485-499 (1976)

Page, F. C.

The genera and possible relationships of the family Amoebidae, with special
attention to comparative ultrastructure.

Protistologica **22**, 301-316 (1986)

Pollard, T. D.

The cytoskeleton, cellular motility and the reductionist agenda.

Nature **422**, 741-5 (2003)

Rinaldi, R. and Opas, M.

Graphs of contracting glycerinated *Amoeba proteus*.

Nature **260**, 522-526 (1976)

Seravin, L. N.

Critical survey of the modern concept of amoeboid movement.

Tsitologiya. **61**, 653-667 (1964)

Sesaki, H. and Ogihara, S.

Protrusion of cell surface coupled with single exocytotic events of secretion of
the slime in Physarum plasmodia.

J. Cell Sci. **110**, 809-18 (1997).

Stockem W.

Pinocytosis and motility of amoeba. I. Influence of marker substances on
Amoeba proteus.

Z. Zellforsch. Mikrosk. Anat. **74**, 372-400 (1966)

Stockem, W. and Korohoda, W.

Effects of induced pinocytotic activity and extreme temperatures on the

morphology of Golgi bodies in *Amoeba proteus*.
Cell Tissue Res. **157**, 541-52 (1975)

Stockem, W.
Pinocytosis and Locomotion of Amoebae III. The Function of the Golgi Apparatus of *Amoeba proteus* and *Chaos chaos*.
Histochemie **18**, 217-240 (1969).

Stockem, W.
Membrane-turnover during locomotion of *Amoeba proteus*.
Acta Protozool. **11**, 83-89 (1972).

Svitkina, T.M and Borisy, G. G.
Arp2/3 complex and actin depolymerizing factor/cofilin in dendritic organization and treadmilling of actin filament array in lamellipodia.
J. Cell Biol. **145**, 1009-26 (1999)

Taylor, D. L., Moore, P. L. and Allen, R. D.
Contractile basis of amoeboid movement. I. the chemical control of motility in isolated cytoplasm.
J. Cell Biol. **59**, 378-394 (1973)

Wohlfarth-Bottermann, K. E. and Stockem, W.
Pinocytose und Bewegung von Amöben
Z. Zellforsch. Mikrosk. Anat. **73**, 444-474 (1966).

Yoshida, K and Soldati, T.
Dissection of amoeboid movement into two mechanically distinct modes.
J. Cell Sci. **119**, 3833-3844 (2006).

Acknowledgement

I am especially grateful to Prof. Teruo Shimmen, Prof. Tohru Yoshihisa, A. prof. Seiji Sonobe, and Dr. Etsuo Yokota (University of Hyogo) for their suggestion about my works. I am very grateful to A. prof. Shigenori Nonaka, Ms. Hiroko Kobayashi (National Institute for Basic Biology) and Dr. Daisuke Takao (University of Michigan) for kind support of using DSLM, and Prof. Yoshinobu Mineyuki (University of Hyogo) and Dr. Daisuke Tamaoki (Kagawa University) for kind support of using spinning-disk confocal microscopy. I want to thank A. prof. Takashi Murata (National Institute for Basic Biology) for kind discussion about spinning-disk microscopy, and Prof. Takashi Osumi and Prof. Tomitake Tsukihara (University of Hyogo) for helpful advice. Special thanks to the late A. prof. Hitoshi Yagisawa (University of Hyogo) for in-depth discussion about protozoa.